

TUM-HEP-448/01
 hep-ph/0112305
 December 2001

QCD Corrections to $\bar{B} \rightarrow X_{d,s}\nu\bar{\nu}$, $\bar{B}_{d,s} \rightarrow l^+l^-$, $K \rightarrow \pi\nu\bar{\nu}$ and $K_L \rightarrow \mu^+\mu^-$ in the MSSM

Christoph Bobeth*, Andrzej J. Buras†, Frank Krüger‡, Jörg Urban§

*Physik Department, Technische Universität München,
 D-85748 Garching, Germany*

Abstract

We compute for the first time QCD corrections to the rare decays $\bar{B} \rightarrow X_{d,s}\nu\bar{\nu}$, $\bar{B}_{d,s} \rightarrow l^+l^-$, $K \rightarrow \pi\nu\bar{\nu}$ and $K_L \rightarrow \mu^+\mu^-$, where $l = e$ or μ , in the context of a supersymmetric extension of the Standard Model (SM) with minimal flavour violation and new operators, in addition to those present in the SM. Assuming that the gluino is heavy, we consider an effective theory which consists of charged and neutral Higgs particles, charginos and squarks. We evaluate the QCD corrections to box and Z^0 -penguin diagrams with top-quark, charged Higgs boson, chargino and squark exchanges, as well as to neutral Higgs boson penguin diagrams. We provide a compendium of analytic formulae for the Wilson coefficients, which are valid for arbitrary values of $\tan\beta$ (the ratio of the vacuum expectation values of the two Higgs fields) except for the case of the neutral Higgs-boson contributions. These contributions have been obtained at large $\tan\beta$, which may compensate for the inevitable suppression by the masses of the light leptons in decays based on the $b \rightarrow s(d)l^+l^-$ transition. We investigate the dependence of the various branching ratios on the renormalization scale μ , which is the main theoretical uncertainty in the short-distance calculation. We find that the μ dependence of the branching ratios is considerably reduced once the QCD corrections are taken into account. The contributions of new operators are found to be dominant at large $\tan\beta$ in $\bar{B}_{d,s} \rightarrow \mu^+\mu^-$ while they are subleading in $\bar{B} \rightarrow X_{d,s}\nu\bar{\nu}$ and completely negligible in kaon decays.

*E-mail address: bobeth@ph.tum.de

†E-mail address: aburas@ph.tum.de

‡E-mail address: fkrueger@ph.tum.de

§E-mail address: urban@ph.tum.de

1 Introduction

The rare decays $\bar{B} \rightarrow X_{d,s}\nu\bar{\nu}$, $\bar{B}_{d,s} \rightarrow l^+l^-$, $K^+ \rightarrow \pi^+\nu\bar{\nu}$ and $K_L \rightarrow \pi^0\nu\bar{\nu}$, where l denotes a lepton, are very promising probes of flavour physics within the Standard Model (SM) and possible extensions, since they are governed essentially by short-distance interactions. (For recent reviews of rare K and B decays, see Refs. [1–4].) These decays are sensitive to the quantum structure of flavour dynamics and can at the same time be computed to an exceptionally high degree of precision. This is due to the fact that (a) the required low energy hadronic matrix elements are just the matrix elements of quark currents between hadron states, which can be extracted from semileptonic decays, including isospin-breaking effects [5]; (b) other long-distance contributions have been found to be negligible [6]; and (c) the contributions of higher dimensional operators turn out to be tiny in the case of $K_L \rightarrow \pi^0\nu\bar{\nu}$ [7], and are below 5% of the charm contribution in the case of $K^+ \rightarrow \pi^+\nu\bar{\nu}$ [8].

As a consequence, the scale ambiguities inherent in perturbative QCD constitute the dominant theoretical uncertainties present in the analysis of the above decay modes. Within the SM, these theoretical uncertainties have been considerably reduced through the inclusion of the next-to-leading order QCD corrections [9–13].

In the decay $K_L \rightarrow \mu^+\mu^-$, on the other hand, there are sizable long-distance contributions associated with a two-photon intermediate state, in addition to the short-distance interaction $d\bar{s} \rightarrow \mu^+\mu^-$. While the absorptive contribution with real photons can be determined by means of the measured $K_L \rightarrow \gamma\gamma$ branching ratio [14], the numerical predictions for the dispersive part of the amplitude due to off-shell photons suffer from theoretical uncertainties inherent in the models for the form factors [15]. We therefore content ourselves with the short-distance part of $K_L \rightarrow \mu^+\mu^-$.

In the context of the minimal supersymmetric standard model (MSSM) [16, 17], the branching ratios for rare B -meson and kaon decays such as $\bar{B} \rightarrow X_s\nu\bar{\nu}$, $\bar{B}_s \rightarrow \mu^+\mu^-$, $K_L \rightarrow \pi^0\nu\bar{\nu}$, $K^+ \rightarrow \pi^+\nu\bar{\nu}$ and $K_L \rightarrow \mu^+\mu^-$ have been considered by many authors (see, e.g., Refs. [18–28]); however, these decay modes have hitherto been studied without the inclusion of QCD corrections. Working in the framework of the SM operator basis, a compendium of the relevant formulae in the limit of degenerate squarks of the first two generations, and valid only for small $\tan\beta$ (the ratio of the vacuum expectation values of the two Higgs fields), has been presented in Ref. [21]. Taking into account all presently available constraints on the supersymmetric parameters, the phenomenological analysis of [21] shows that the supersymmetric contributions to the above-mentioned processes can be quite substantial. Indeed, denoting the MSSM prediction for a given decay normalized to the SM result by R , and setting all the SM parameters that are unaffected by supersymmetric contributions at their central values, one finds the following ranges¹

$$0.73 \leq R(\bar{B} \rightarrow X_s\nu\bar{\nu}) \leq 1.34, \quad 0.68 \leq R(\bar{B}_s \rightarrow \mu^+\mu^-) \leq 1.53, \quad (1.1)$$

¹Note that these ranges become larger once the SM parameters are varied.

$$0.65 \leq R(K^+ \rightarrow \pi^+ \nu \bar{\nu}) \leq 1.02, \quad 0.41 \leq R(K_L \rightarrow \pi^0 \nu \bar{\nu}) \leq 1.03. \quad (1.2)$$

Clearly, in view of large parametric uncertainties related to the SM parameters and the masses of the supersymmetric particles, precise predictions for the above branching ratios are not possible at present. Nevertheless, the situation may change considerably in this decade due to the improved determination of the SM parameters in forthcoming B - and K -physics dedicated experiments, as well as through an anticipated discovery of supersymmetric particles. Besides, all the branching ratios considered in this paper could conceivably be measured in this decade. We think that these prospects, together with the theoretical cleanliness of these decays, justify a more accurate computation of the relevant branching ratios in the MSSM.

In this paper, we extend existing calculations in two ways:

- (i) We compute for the first time QCD corrections to the branching ratios of $\bar{B} \rightarrow X_{d,s} \nu \bar{\nu}$, $\bar{B}_{d,s} \rightarrow l^+ l^-$, $K^+ \rightarrow \pi^+ \nu \bar{\nu}$, $K_L \rightarrow \pi^0 \nu \bar{\nu}$ and $K_L \rightarrow \mu^+ \mu^-$, within supersymmetry (SUSY).
- (ii) We also include the contributions of new operators beyond those present in the SM.

While such an enterprise would have been a formidable task ten years ago, it is a relatively straightforward computation by means of analytic computer programs developed during the last five years.

It is the main objective of the present work to investigate the dependence of the various branching ratios on the renormalization scale μ within SUSY, taking into account QCD corrections. As we shall see, the inclusion of these corrections will significantly reduce the unphysical renormalization scale dependence of the branching ratios originating in the scale dependence of the running quark and squark masses.

In the quantitative analysis, we focus on the two distinctly different regions

$$2 \leq \tan \beta \leq 5, \quad 40 \leq \tan \beta \leq 60, \quad (1.3)$$

which we refer to as the low and high $\tan \beta$ regime, respectively. Our results for the Wilson coefficients that will be presented below are valid for arbitrary values of $\tan \beta$, except for the neutral Higgs-boson contributions, which are sizable only in the high $\tan \beta$ regime for the decays under study.

The outline of this paper is as follows. In Sec. 2, we touch on the elements of the MSSM and define our notation. Section 3 is a compendium of the relevant effective Hamiltonians and the corresponding Wilson coefficients including $\mathcal{O}(\alpha_s)$ corrections, in the context of the MSSM. In Sec. 4, we give technical details of our calculation of the QCD corrections. In Sec. 5, we present a collection of the branching ratios in question. Section 6 is devoted to the numerical analysis, which is based on the assumption of minimal flavour violation and performed in the low as well as the high $\tan \beta$ regime. Some comments on the SUSY QCD corrections to the b quark Yukawa coupling, relevant at large $\tan \beta$, will be made in Sec. 7. Finally, in Sec. 8, we summarize and conclude. A compilation of the various loop functions is given in the Appendices.

2 Couplings and mixing matrices in the MSSM

We start by introducing the relevant mass and mixing matrices in the context of SUSY with minimal particle content and R -parity conservation, which we will call the minimal supersymmetric standard model (MSSM). In the numerical analysis, we confine ourselves to a version of the model with minimal flavour violation, i.e., we assume that flavour mixing is due exclusively to the Cabibbo-Kobayashi-Maskawa (CKM) matrix. In addition, we take the down squark mass-squared matrix to be flavour diagonal, so that there are no neutralino contributions.

The MSSM is usually embedded in a grand unified theory (GUT) in order to solve the problem with too large contributions to flavour-changing neutral currents and to further reduce the vast number of unknown parameters. This leads to the minimal supergravity inspired model in which one assumes universality of the soft terms at the scale of gauge coupling unification, say, M_{GUT} . Renormalization group effects then induce flavour off-diagonal entries, e.g., in the squark mass-squared matrices at the electroweak scale. In our numerical analysis, however, we do not relate the soft SUSY-breaking parameters to some common high scale, but rather take them at the electroweak scale while discarding flavour off-diagonal terms in the squark mass-squared matrix.

2.1 Chargino mass matrix

The chargino mass matrix is given by

$$M_{\tilde{\chi}} = \begin{pmatrix} M_2 & \sqrt{2}M_W \sin \beta \\ \sqrt{2}M_W \cos \beta & \mu \end{pmatrix}, \quad (2.1)$$

where M_2 and μ are the W -ino and Higgsino mass parameters, respectively. This matrix can be cast in diagonal form by means of a biunitary transformation

$$U^* M_{\tilde{\chi}} V^\dagger = \text{diag}(M_{\tilde{\chi}_1}, M_{\tilde{\chi}_2}), \quad (2.2)$$

$M_{\tilde{\chi}_{1,2}}$ being the chargino masses with $M_{\tilde{\chi}_1}^2 < M_{\tilde{\chi}_2}^2$. The analytic expressions for $M_{\tilde{\chi}_{1,2}}$ and the matrices U, V can be found in Ref. [29].

2.2 Squark mass matrix

It proves convenient to work in the super-CKM basis [30], in which the quark mass matrices are diagonal, and both quarks and squarks are rotated simultaneously. Denoting up-type squarks by \tilde{U} , the 6×6 mass-squared matrix in the $(\tilde{U}_L, \tilde{U}_R)$ basis is given by

$$M_{\tilde{U}}^2 = \begin{pmatrix} M_{\tilde{U}_L}^2 + M_U^2 + M_Z^2 \cos 2\beta (\frac{1}{2} - \frac{2}{3} \sin^2 \theta_W) \mathbb{1} & M_U (A_U^* - \mu \cot \beta \mathbb{1}) \\ M_U (A_U - \mu^* \cot \beta \mathbb{1}) & M_{\tilde{U}_R}^2 + M_U^2 + \frac{2}{3} M_Z^2 \cos 2\beta \sin^2 \theta_W \mathbb{1} \end{pmatrix}, \quad (2.3)$$

where θ_W is the Weinberg angle, $M_{\tilde{U}_{L,R}}$ are the soft SUSY breaking up-type squark mass matrices, $M_U \equiv \text{diag}(m_u, m_c, m_t)$, A_U contains the trilinear soft SUSY-breaking parameters and $\mathbb{1}$ represents the unit matrix. The matrix $M_{\tilde{U}}^2$ can be diagonalized by a unitary matrix Γ^U such that

$$\Gamma^U M_{\tilde{U}}^2 \Gamma^{U\dagger} = \text{diag}(m_{\tilde{u}_1}^2, m_{\tilde{u}_2}^2, \dots, m_{\tilde{u}_6}^2). \quad (2.4)$$

For later use it is convenient to define the 6×3 matrices

$$(\Gamma^{U_L})_{ai} = (\Gamma^U)_{ai}, \quad (\Gamma^{U_R})_{ai} = (\Gamma^U)_{a,i+3}. \quad (2.5)$$

2.3 Slepton mass matrices

Similarly to the mixing matrix for the squarks, we define the matrices Γ^E in the charged slepton sector through

$$\Gamma^E M_{\tilde{l}}^2 \Gamma^{E\dagger} = \text{diag}(m_{\tilde{l}_1}^2, m_{\tilde{l}_2}^2, \dots, m_{\tilde{l}_6}^2), \quad (2.6)$$

with the mass-squared matrix, in the super-CKM basis,

$$M_{\tilde{l}}^2 = \begin{pmatrix} M_{\tilde{l}_L}^2 + M_E^2 - \frac{1}{2}M_Z^2 \cos 2\beta(1 - 2 \sin^2 \theta_W) \mathbb{1} & M_E(A_l^* - \mu \tan \beta \mathbb{1}) \\ M_E(A_l - \mu^* \tan \beta \mathbb{1}) & M_{\tilde{l}_R}^2 + M_E^2 - M_Z^2 \cos 2\beta \sin^2 \theta_W \mathbb{1} \end{pmatrix}, \quad (2.7)$$

where $M_{\tilde{l}_{L,R}}$ are the soft SUSY breaking charged slepton mass matrices, $M_E \equiv \text{diag}(m_e, m_\mu, m_\tau)$ and A_l contains the soft SUSY breaking trilinear couplings. As before, we introduce the 6×3 mixing matrices

$$(\Gamma^{E_L})_{ai} = (\Gamma^E)_{ai}, \quad (\Gamma^{E_R})_{ai} = (\Gamma^E)_{a,i+3}. \quad (2.8)$$

Finally, if we assume the neutrinos to be massless, we are left with the 3×3 mixing matrix Γ^N in the sneutrino sector, which is defined by

$$\Gamma^N M_{\tilde{\nu}}^2 \Gamma^{N\dagger} = \text{diag}(m_{\tilde{\nu}_1}^2, m_{\tilde{\nu}_2}^2, m_{\tilde{\nu}_3}^2), \quad (2.9)$$

where the sneutrino mass-squared matrix reads

$$M_{\tilde{\nu}}^2 = M_{\tilde{l}_L}^2 + \frac{1}{2}M_Z^2 \cos 2\beta \mathbb{1}. \quad (2.10)$$

2.4 Interactions within the MSSM

Recalling

$$P_{L,R} = (1 \mp \gamma_5)/2, \quad g = e/\sin \theta_W, \quad g_s^2 = 4\pi\alpha_s, \\ M_U \equiv \text{diag}(m_u, m_c, m_t), \quad M_E \equiv \text{diag}(m_e, m_\mu, m_\tau), \quad M_D \equiv \text{diag}(m_d, m_s, m_b), \quad (2.11)$$

the relevant interaction vertices of the MSSM with decoupled gluinos and massless neutrinos in the super-CKM basis can be written as²

$$\mathcal{L}_H = \frac{g}{\sqrt{2}M_W} [\cot \beta (\bar{u} M_U V_{\text{CKM}} P_L d) + \tan \beta (\bar{u} V_{\text{CKM}} M_D P_R d)] H^+ + \text{H.c.}, \quad (2.12)$$

$$\mathcal{L}_{\tilde{\chi}} = \sum_{i=1}^2 \left\{ \overline{\tilde{\chi}_i^-} [\tilde{\nu}^\dagger (X_i^{N_L} P_L + X_i^{N_R} P_R) l + \tilde{u}^\dagger (X_i^{U_L} P_L + X_i^{U_R} P_R) d] \right. \\ \left. + \overline{\tilde{\chi}_i^+} [\tilde{l}^\dagger (X_i^{E_L} P_L + X_i^{E_R} P_R) \nu] \right\} + \text{H.c.}, \quad (2.13)$$

$$\mathcal{L}_{\tilde{\chi}\tilde{\chi}Z} = \frac{g \sec \theta_W}{2} \sum_{i,j=1}^2 \overline{\tilde{\chi}_i^-} \gamma^\mu (U_{i1} U_{j1}^* P_L + V_{i1}^* V_{j1} P_R + \cos 2\theta_W \delta_{ij}) \tilde{\chi}_j^- Z_\mu^0, \quad (2.14)$$

$$\mathcal{L}_{\tilde{u}\tilde{u}Z} = -\frac{ig \sec \theta_W}{2} \left[(\Gamma^{U_L} \Gamma^{U_L \dagger})_{ab} - \frac{4}{3} \sin^2 \theta_W \delta_{ab} \right] (\tilde{u}_a^* \overset{\leftrightarrow}{\partial}^\mu \tilde{u}_b) Z_\mu^0, \quad (2.15)$$

$$\mathcal{L}_4 \equiv \mathcal{L}_{\tilde{u}\tilde{u}\tilde{u}\tilde{u}}^{g_s} = -\frac{1}{2} g_s^2 (\tilde{u}^* P_U T^c \tilde{u})^2, \quad (2.16)$$

where

$$X_i^{U_L} = -g \left[a_g V_{i1}^* \Gamma^{U_L} - a_Y V_{i2}^* \Gamma^{U_R} \frac{M_U}{\sqrt{2}M_W \sin \beta} \right] V_{\text{CKM}}, \quad (2.17)$$

$$X_i^{U_R} = g a_Y U_{i2} \Gamma^{U_L} V_{\text{CKM}} \frac{M_D}{\sqrt{2}M_W \cos \beta}, \quad (2.18)$$

$$X_i^{N_L} = -g V_{i1}^* \Gamma^N, \quad X_i^{N_R} = g U_{i2} \Gamma^N \frac{M_E}{\sqrt{2}M_W \cos \beta}, \quad (2.19)$$

$$X_i^{E_L} = -g \left[U_{i1}^* \Gamma^{E_L} - U_{i2}^* \Gamma^{E_R} \frac{M_E}{\sqrt{2}M_W \cos \beta} \right], \quad X_i^{E_R} = 0, \quad (2.20)$$

²For simplicity of presentation, we suppress the generation indices. Furthermore, we define the charginos $\tilde{\chi}_i^-$ ($i = 1, 2$) as particles, contrary to Refs. [17, 30, 31], with $\tilde{\chi}_i^+ \equiv (\tilde{\chi}_i^-)^c$.

$$P_U \equiv \Gamma^{U_L} \Gamma^{U_L^\dagger} - \Gamma^{U_R} \Gamma^{U_R^\dagger}. \quad (2.21)$$

In these equations, V_{CKM} is the CKM matrix and T^c ($c = 1, \dots, 8$) are the generators of colour gauge symmetry. The mixing matrices $U, V, \Gamma^{U_{L,R}}$ and $\Gamma^{E_{L,R}}$ are defined through Eqs. (2.2), (2.5) and (2.8), respectively, and the 3×3 sneutrino mixing matrix Γ^N is defined via Eq. (2.9).

The effect of the decoupled gluino, with mass $M_{\tilde{g}}$, is contained in the functions a_g and a_Y [32], which are given by

$$a_g = 1 - \frac{\alpha_s(\mu)}{4\pi} \left[\frac{7}{3} + 2 \ln \left(\frac{\mu^2}{M_{\tilde{g}}^2} \right) \right], \quad a_Y = 1 + \frac{\alpha_s(\mu)}{4\pi} \left[1 + 2 \ln \left(\frac{\mu^2}{M_{\tilde{g}}^2} \right) \right], \quad (2.22)$$

μ being the matching scale which will be discussed in more detail at the end of Sec. 3.³

As for the couplings of the neutral Higgs bosons, we refer to [31].

2.5 Tree-level relations within the MSSM

In calculating the neutral Higgs-boson contributions, we shall exploit the tree-level relations

$$M_{A^0}^2 = M_H^2 - M_W^2, \quad (2.23)$$

$$M_{h^0, H^0}^2 = \frac{1}{2} \{ M_{A^0}^2 + M_Z^2 \mp [(M_{A^0}^2 + M_Z^2)^2 - 4M_Z^2 M_{A^0}^2 \cos^2 2\beta]^{1/2} \}, \quad (2.24)$$

$$\sin 2\alpha = -\sin 2\beta \left(\frac{M_{H^0}^2 + M_{h^0}^2}{M_{H^0}^2 - M_{h^0}^2} \right), \quad (2.25)$$

where M_H and M_{A^0} are the masses of the charged and CP-odd Higgs boson, respectively, and M_{h^0, H^0} and α are the masses and mixing angle in the CP-even Higgs sector. Thus, at the tree-level, the Higgs sector of the MSSM is described by merely two free parameters that we choose to be $\tan \beta$ and M_H . Since the results that will be presented in the next section have been obtained at leading order in the electroweak couplings, the tree-level relations are quite adequate for our purposes.

3 Effective Hamiltonians and Wilson coefficients

3.1 Notation

Within the context of the SM and the two-Higgs-doublet model (2HDM), as well as the MSSM, at low $\tan \beta$, only a small number of operators contribute to the decays under study, and the Wilson

³Equation (2.22) can be obtained from the result of Ref. [33] by performing the limit $M_{\tilde{g}} \rightarrow \infty$.

coefficients can be expressed in terms of only two functions usually denoted by X and Y [1, 9–13] (see Appendix A for the SM result).

For large values of $\tan \beta$, on the other hand, significant contributions of new operators are conceivable and such a convenient notation is no longer applicable. In fact, since a given Z^0 -penguin or box diagram with a certain particle exchange ($W^\pm, H^\pm, \tilde{\chi}^\pm$) can contribute to the coefficients of several operators, it is useful to proceed as follows:

- All Z^0 -penguin contributions are included in the functions $C^{\nu\bar{\nu}}$ and $C^{l\bar{l}}$ which describe the processes $b \rightarrow q\nu\bar{\nu}$ and $b \rightarrow ql^+l^-$ ($q = d, s$), respectively. Likewise, the box-diagram contributions are expressed in terms of the functions $B^{\nu\bar{\nu}}$ and $B^{l\bar{l}}$.
- In the case of the $b \rightarrow ql^+l^-$ transition, there may be sizable contributions due to neutral Higgs boson penguin diagrams at large $\tan \beta$, leading to the function $N^{l\bar{l}}$.
- Owing to quartic squark vertices, there are additional contributions to Z^0 -penguin, box- and penguin diagrams with neutral Higgs bosons. Indeed, when the running mass of the squarks in the modified minimal subtraction ($\overline{\text{MS}}$) scheme is used, diagrams involving quartic squark couplings have to be included. As we shall discuss in Sec. 4, these contributions vanish after renormalization when the pole mass of the squarks is used instead. Below, these contributions will be labelled by the index $J = 4$.
- The results obtained in the B sector can be easily altered to apply to the kaon system.
- Including QCD corrections, and denoting the SM, charged Higgs-boson, chargino and ‘quartic’ contributions by $J = \text{SM}, H, \tilde{\chi}, 4$, the functions mentioned above have the structure ⁴

$$[C_I^{\nu\bar{\nu}}]_J = [C_I^{\nu\bar{\nu}}]_J^{(0)} + \frac{\alpha_s}{4\pi} [C_I^{\nu\bar{\nu}}]_J^{(1)}, \quad [C_I^{l\bar{l}}]_J = [C_I^{l\bar{l}}]_J^{(0)} + \frac{\alpha_s}{4\pi} [C_I^{l\bar{l}}]_J^{(1)}, \quad (3.1a)$$

$$[B_I^{\nu\bar{\nu}}]_J = [B_I^{\nu\bar{\nu}}]_J^{(0)} + \frac{\alpha_s}{4\pi} [B_I^{\nu\bar{\nu}}]_J^{(1)}, \quad [B_I^{l\bar{l}}]_J = [B_I^{l\bar{l}}]_J^{(0)} + \frac{\alpha_s}{4\pi} [B_I^{l\bar{l}}]_J^{(1)}, \quad (3.1b)$$

$$[N_I^{l\bar{l}}]_J = [N_I^{l\bar{l}}]_J^{(0)} + \frac{\alpha_s}{4\pi} [N_I^{l\bar{l}}]_J^{(1)}, \quad (3.1c)$$

where the subscript I indicates the various operators, which will be discussed shortly. Note that there are no sizable neutral Higgs-boson contributions within the SM as they are invariably suppressed by the light fermion masses, and hence can be safely neglected.

⁴Recall that in our scenario (i) the gluino decouples, and (ii) there are no neutralino contributions since we assume the down squark mass-squared matrix to be flavour diagonal.

- Finally, we define the mass ratios

$$x = \frac{m_t^2}{M_W^2}, \quad y = \frac{m_t^2}{M_H^2}, \quad z = \frac{M_H^2}{M_W^2}, \quad (3.2a)$$

$$x_{ij} = \frac{M_{\tilde{\chi}_i}^2}{M_{\tilde{\chi}_j}^2}, \quad y_{ai} = \frac{m_{\tilde{u}_a}^2}{M_{\tilde{\chi}_i}^2}, \quad z_{bi} = \frac{m_{\tilde{l}_b}^2}{M_{\tilde{\chi}_i}^2}, \quad v_{fi} = \frac{m_{\tilde{\nu}_f}^2}{M_{\tilde{\chi}_i}^2}, \quad (3.2b)$$

and introduce the abbreviations

$$s_W \equiv \sin \theta_W, \quad L_t \equiv \ln \left(\frac{\mu^2}{m_t^2} \right), \quad L_{\tilde{u}_a} \equiv \ln \left(\frac{\mu^2}{m_{\tilde{u}_a}^2} \right), \quad \kappa_q \equiv \frac{1}{8\sqrt{2}G_F e^2 V_{tb} V_{tq}^*}. \quad (3.2c)$$

3.2 The $b \rightarrow s(d)\nu\bar{\nu}$ transition

Let us start with the effective Hamiltonian describing the $b \rightarrow q\nu_f\bar{\nu}_f$ transition, where $q = d, s$ and $f = e, \mu, \tau$. Within the SM, it is given by⁵

$$\mathcal{H}_{\text{eff}}^f = \frac{4G_F}{\sqrt{2}} \frac{\alpha}{2\pi \sin^2 \theta_W} \sum_{i=u,c,t} V_{ib} V_{iq}^* \tilde{c}_L^i(m_i) (\bar{q} \gamma_\mu P_L b) (\bar{\nu}_f \gamma^\mu P_L \nu_f), \quad (3.3)$$

where $\tilde{c}_L^i(m_i)$ represent the contributions from internal quarks $i = u, c, t$, and m_i are the corresponding masses. Using the unitarity of the CKM matrix, the effective Hamiltonian can be written as

$$\begin{aligned} \mathcal{H}_{\text{eff}}^f &= \frac{4G_F}{\sqrt{2}} \frac{\alpha}{2\pi \sin^2 \theta_W} \sum_{i=c,t} V_{ib} V_{iq}^* [\tilde{c}_L^i(m_i) - \tilde{c}_L^u(m_u)] (\bar{q} \gamma_\mu P_L b) (\bar{\nu}_f \gamma^\mu P_L \nu_f) \\ &= \frac{4G_F}{\sqrt{2}} \frac{\alpha}{2\pi \sin^2 \theta_W} \sum_{i=c,t} V_{ib} V_{iq}^* c_L^i(m_i) (\bar{q} \gamma_\mu P_L b) (\bar{\nu}_f \gamma^\mu P_L \nu_f), \end{aligned} \quad (3.4)$$

with $c_L^i(0) = 0$. [Note that in the second line of Eq. (3.4) we have taken the limit $m_u \rightarrow 0$.]

Exploiting the fact that

$$\frac{c_L^c(m_c)}{c_L^t(m_t)} \sim O(10^{-3}), \quad \left| \frac{V_{cb} V_{cq}^*}{V_{tb} V_{tq}^*} \right| \sim O(1) \quad (q = d, s), \quad (3.5)$$

the charm-quark contribution to the quark-level process $b \rightarrow q\nu_f\bar{\nu}_f$ can be safely neglected, and we arrive at

$$\mathcal{H}_{\text{eff}}^f = \frac{4G_F}{\sqrt{2}} \frac{\alpha}{2\pi \sin^2 \theta_W} V_{tb} V_{tq}^* c_L^t(m_t) (\bar{q} \gamma_\mu P_L b) (\bar{\nu}_f \gamma^\mu P_L \nu_f). \quad (3.6)$$

⁵Throughout this paper, we suppress the neutrino flavour index f carried by the Wilson coefficients.

The extension of this result to a non-standard operator basis is straightforward. Henceforth, we will omit the superscript t of the Wilson coefficient in Eq. (3.6).

Assuming that the neutrinos are essentially massless, and hence purely left-handed, the effective Hamiltonian in the presence of new operators has the particularly simple form

$$\mathcal{H}_{\text{eff}} = \frac{4G_F}{\sqrt{2}} \frac{\alpha}{2\pi \sin^2 \theta_W} V_{tb} V_{tq}^* \sum_{f=e,\mu,\tau} [c_L \mathcal{O}_L + c_R \mathcal{O}_R], \quad (3.7)$$

where

$$\mathcal{O}_L = (\bar{q} \gamma_\mu P_L b)(\bar{\nu}_f \gamma^\mu P_L \nu_f), \quad \mathcal{O}_R = (\bar{q} \gamma_\mu P_R b)(\bar{\nu}_f \gamma^\mu P_R \nu_f), \quad (3.8)$$

and the short-distance coefficients

$$c_L = \sum_{J=\text{SM},H,\tilde{\chi},4} \{[C_L^{\nu\bar{\nu}}]_J + [B_L^{\nu\bar{\nu}}]_J\}, \quad c_R = \sum_{J=\text{SM},H,\tilde{\chi},4} \{[C_R^{\nu\bar{\nu}}]_J + [B_R^{\nu\bar{\nu}}]_J\}. \quad (3.9)$$

Note that the Wilson coefficients of tensor and scalar operators such as $(\bar{q} \sigma^{\mu\nu} P_{L,R} b)(\bar{\nu} \sigma_{\mu\nu} P_{L,R} \nu)$ and $(\bar{q} P_{L,R} b)(\bar{\nu} P_{L,R} \nu)$ vanish for massless neutrinos in the final state.

3.2.1 Z^0 -penguin contributions

The QCD corrections to the Wilson coefficients are calculated from the Feynman diagrams in Figs. 1 and 2, while those involving the quartic squark couplings are depicted in Fig. 3. Recalling the definitions in Eqs. (3.2), we find

$$[C_L^{\nu\bar{\nu}}]_{\text{SM}} = \frac{1}{4} \left\{ f_1^{(0)}(x) + \frac{\alpha_s}{4\pi} \left[f_1^{(1)}(x) + 8x \frac{\partial}{\partial x} f_1^{(0)}(x) L_t \right] \right\}, \quad (3.10)$$

$$[C_R^{\nu\bar{\nu}}]_{\text{SM}} = 0, \quad (3.11)$$

$$[C_L^{\nu\bar{\nu}}]_H = -\frac{M_H^2 \cot^2 \beta}{8M_W^2} \left\{ y f_2^{(0)}(y) + \frac{\alpha_s}{4\pi} \left[y f_2^{(1)}(y) + 8y \frac{\partial}{\partial y} [y f_2^{(0)}(y)] L_t \right] \right\}, \quad (3.12)$$

$$[C_R^{\nu\bar{\nu}}]_H = \frac{m_b m_q \tan^2 \beta}{8M_W^2} \left\{ f_2^{(0)}(y) + \frac{\alpha_s}{4\pi} \left[f_2^{(1)}(y) + 8 \left(1 + y \frac{\partial}{\partial y} \right) f_2^{(0)}(y) L_t \right] \right\}, \quad (3.13)$$

$$\begin{aligned} [C_L^{\nu\bar{\nu}}]_{\tilde{\chi}} = & -\frac{\kappa_q e^2}{4M_W^2} \sum_{i,j=1}^2 \sum_{a,b=1}^6 (X_j^{U_L\dagger})_{qb} (X_i^{U_L})_{a3} \\ & \times \left\{ 2\sqrt{x_{ji}} \left\{ f_3^{(0)}(x_{ji}, y_{ai}) + \frac{\alpha_s}{4\pi} \left[f_3^{(1)}(x_{ji}, y_{ai}) + 4 \left(1 + y_{ai} \frac{\partial}{\partial y_{ai}} \right) f_3^{(0)}(x_{ji}, y_{ai}) L_{\tilde{u}_a} \right] \right\} U_{j1} U_{i1}^* \delta_{ab} \right. \\ & - \left\{ f_4^{(0)}(x_{ji}, y_{ai}) + \frac{\alpha_s}{4\pi} \left[f_4^{(1)}(x_{ji}, y_{ai}) + 4 \left(1 + y_{ai} \frac{\partial}{\partial y_{ai}} \right) f_4^{(0)}(x_{ji}, y_{ai}) L_{\tilde{u}_a} \right] \right\} V_{j1}^* V_{i1} \delta_{ab} \\ & + \left. \left\{ f_4^{(0)}(y_{ai}, y_{bi}) + \frac{\alpha_s}{4\pi} \left[f_5^{(1)}(y_{ai}, y_{bi}) + 4 \left(1 + y_{ai} \frac{\partial}{\partial y_{ai}} + y_{bi} \frac{\partial}{\partial y_{bi}} \right) f_4^{(0)}(y_{ai}, y_{bi}) L_{\tilde{u}_a} \right] \right\} \right. \\ & \times (\Gamma^{U_L} \Gamma^{U_L\dagger})_{ba} \delta_{ij} \left. \right\}, \quad (3.14) \end{aligned}$$

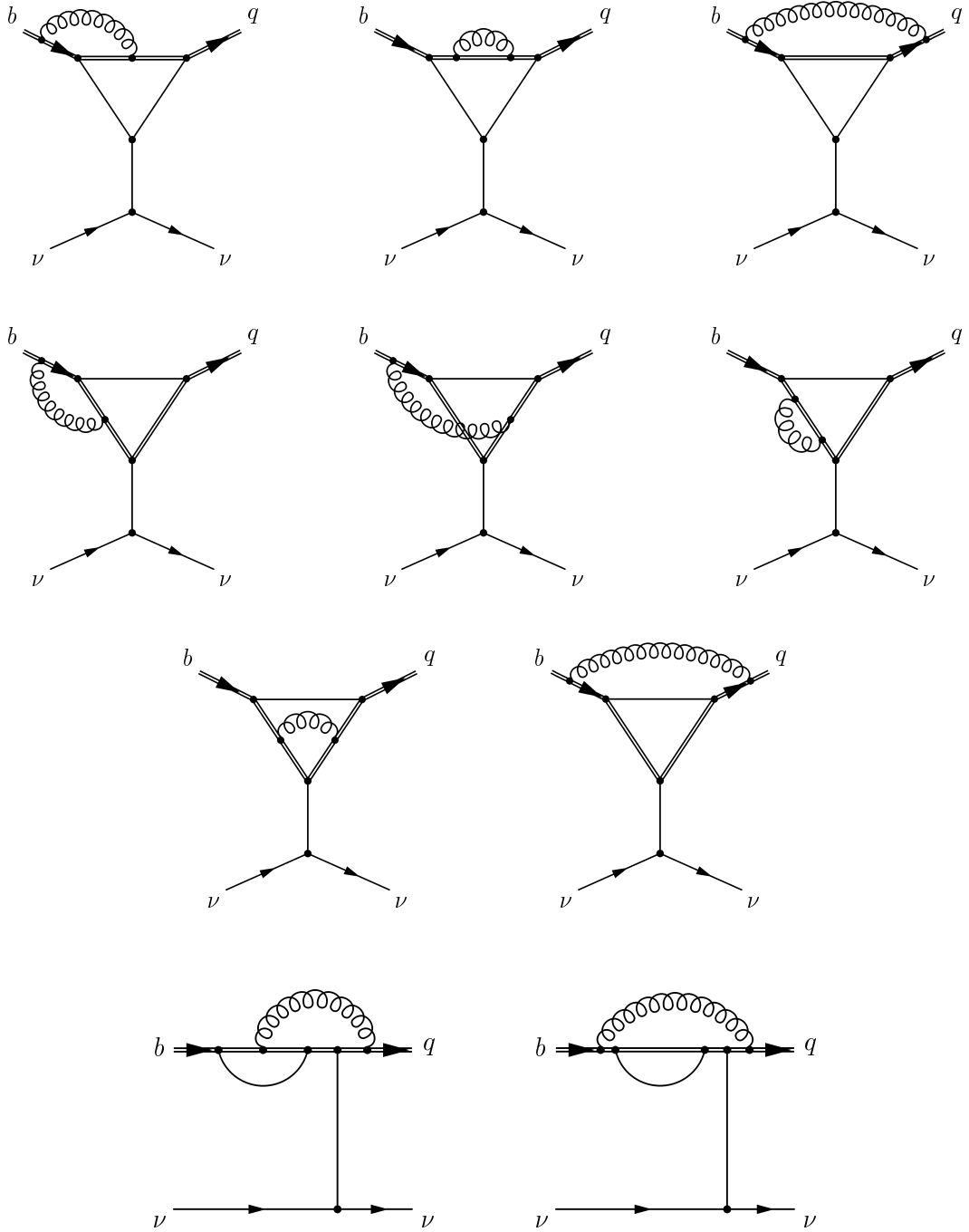


Figure 1: Penguin diagrams contributing to the transition $b \rightarrow q\nu\bar{\nu}$ ($q = d, s$) at order α_s . The vertical and curly lines denote Z^0 bosons and gluons, respectively, while the coloured particles (i.e. quarks and their superpartners) are represented by double lines. The diagrams for $b \rightarrow ql^+l^-$ may be obtained by replacing $\nu \rightarrow l$ and by taking into account neutral Higgs and would-be-Goldstone bosons, in addition to the Z^0 boson. The corresponding symmetric diagrams are not shown here.

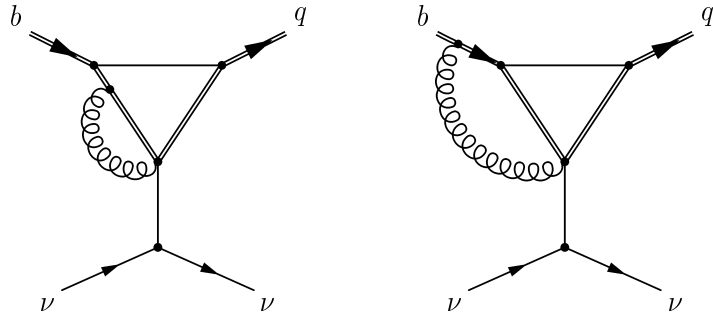


Figure 2: Feynman diagrams with quartic couplings contributing to the decay $b \rightarrow q\nu\bar{\nu}$, $q = d, s$, where the vertical line corresponds to the Z^0 boson. In the case of the $b \rightarrow ql^+l^-$ transition, one simply replaces $\nu \rightarrow l$. We refrain from showing the symmetric vertex corrections here.

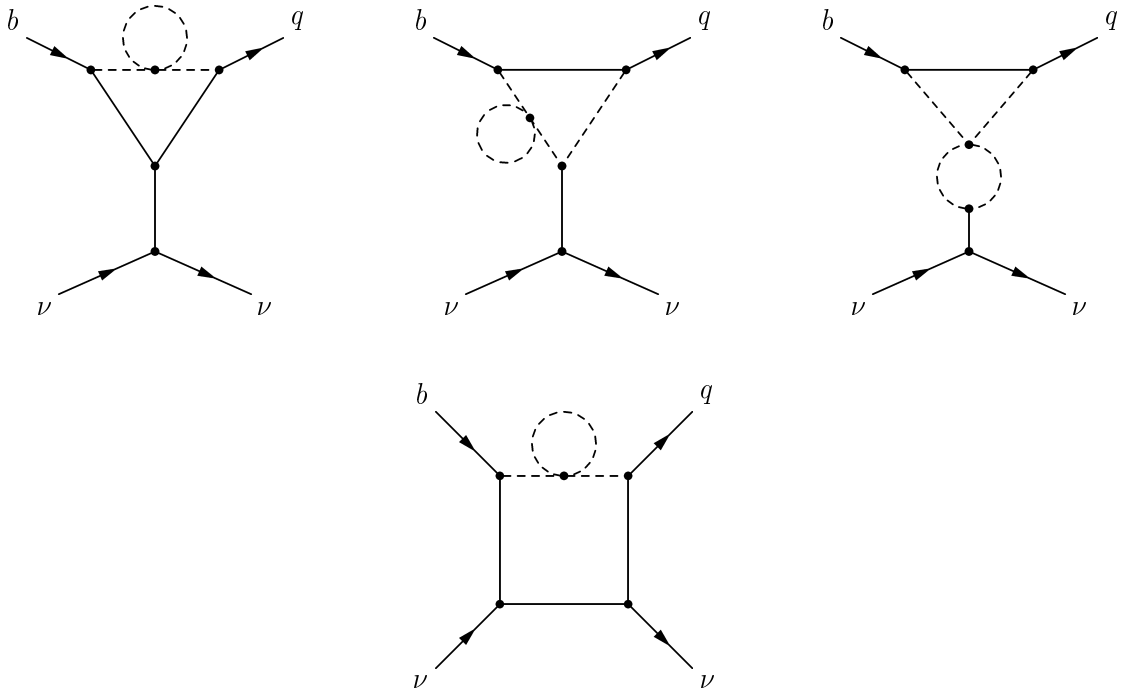


Figure 3: The contributions to the $b \rightarrow q\nu\bar{\nu}$ ($q = d, s$) transition due to quartic squark couplings. The dashed lines denote scalar quarks while the solid lines represent charginos, scalar leptons, and the Z^0 boson. As for the diagrams describing the $b \rightarrow ql^+l^-$ transition, we refer to the captions of Figs. 1 and 4.

$$[C_R^{\nu\bar{\nu}}]_{\tilde{\chi}} = [C_L^{\nu\bar{\nu}}]_{\tilde{\chi}} (X^{U_L} \rightarrow X^{U_R}; U \rightarrow V^*; V \rightarrow U^*; \Gamma^{U_L} \Gamma^{U_L\dagger} \rightarrow -\Gamma^{U_R} \Gamma^{U_R\dagger}), \quad (3.15)$$

$$\begin{aligned} [C_L^{\nu\bar{\nu}}]_4 &= \frac{\alpha_s}{4\pi} \frac{\kappa_q e^2}{6M_W^2} \sum_{i,j=1}^2 \sum_{a,\dots,e,g,k=1}^6 (X_j^{U_L\dagger})_{qd} (X_i^{U_L})_{a3} [(P_U)_{ek} y_{ki} (P_U)_{kg} (1 + L_{\tilde{u}_k})] \\ &\times \left\{ 2\sqrt{x_{ji}} f_6^{(0)}(x_{ji}, y_{ai}, y_{di}) U_{j1} U_{i1}^* \delta_{ae} \delta_{gd} - f_5^{(0)}(x_{ji}, y_{ai}, y_{di}) V_{j1}^* V_{i1} \delta_{ae} \delta_{gd} \right. \\ &\left. + f_5^{(0)}(y_{ai}, y_{bi}, y_{ci}) (\Gamma^{U_L} \Gamma^{U_L\dagger})_{bc} \delta_{ij} \delta_{ae} \delta_{bg} \delta_{cd} + f_5^{(0)}(y_{ai}, y_{ci}, y_{di}) (\Gamma^{U_L} \Gamma^{U_L\dagger})_{bc} \delta_{ij} \delta_{ab} \delta_{ce} \delta_{dg} \right\}, \quad (3.16) \end{aligned}$$

$$[C_R^{\nu\bar{\nu}}]_4 = [C_L^{\nu\bar{\nu}}]_4 (X^{U_L} \rightarrow X^{U_R}; U \rightarrow V^*; V \rightarrow U^*; \Gamma^{U_L} \Gamma^{U_L\dagger} \rightarrow -\Gamma^{U_R} \Gamma^{U_R\dagger}), \quad (3.17)$$

where the index q carried by the $X_i^{U_{L,R}}$ matrices is

$$q = \begin{cases} 1 & \text{for } b \rightarrow d, \\ 2 & \text{for } b \rightarrow s, \end{cases} \quad (3.18)$$

while P_U has already been defined in Eq. (2.21). We should stress that all quark and scalar quark masses entering the above formulae, as well as the expressions that follow, are running masses in the $\overline{\text{MS}}$ scheme, i.e., $m_b \equiv m_b(\mu)$, $m_q \equiv m_q(\mu)$, and so on (see Sec. 3.6 below). The loop functions, $f_p^{(0)}$, $f_p^{(1)}$, are listed in Appendix B.

3.2.2 Box-diagram contributions

The relevant Feynman diagrams, which contribute at $O(\alpha_s)$, are depicted in Figs. 3 and 4. We find

$$[B_L^{\nu\bar{\nu}}]_{\text{SM}} = -f_2^{(0)}(x) - \frac{\alpha_s}{4\pi} \left[f_6^{(1)}(x) + 8x \frac{\partial}{\partial x} f_2^{(0)}(x) L_t \right], \quad (3.19)$$

$$[B_R^{\nu\bar{\nu}}]_{\text{SM}} = 0, \quad (3.20)$$

$$[B_L^{\nu\bar{\nu}}]_H = 0, \quad (3.21)$$

$$[B_R^{\nu\bar{\nu}}]_H = -\frac{m_b m_q m_f^2 \tan^4 \beta}{16 M_H^2 M_W^2} \left\{ f_2^{(0)}(y) + \frac{\alpha_s}{4\pi} \left[f_7^{(1)}(y) + 8 \left(1 + y \frac{\partial}{\partial y} \right) f_2^{(0)}(y) L_t \right] \right\}, \quad (3.22)$$

$$\begin{aligned} [B_L^{\nu\bar{\nu}}]_{\tilde{\chi}} &= \frac{\kappa_q S_W^2}{2} \sum_{i,j=1}^2 \sum_{a,b=1}^6 \frac{1}{M_{\tilde{\chi}_i}^2} (X_j^{E_L})_{bf} (X_i^{E_L\dagger})_{fb} (X_j^{U_L\dagger})_{qa} (X_i^{U_L})_{a3} \left\{ f_5^{(0)}(x_{ji}, y_{ai}, z_{bi}) \right. \\ &\left. + \frac{\alpha_s}{4\pi} \left[f_8^{(1)}(x_{ji}, y_{ai}, z_{bi}) + 4 \left(1 + y_{ai} \frac{\partial}{\partial y_{ai}} \right) f_5^{(0)}(x_{ji}, y_{ai}, z_{bi}) L_{\tilde{u}_a} \right] \right\}, \quad (3.23) \end{aligned}$$

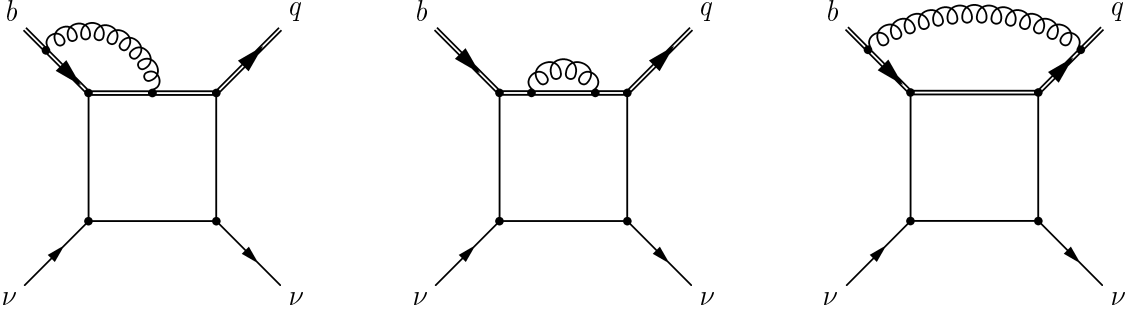


Figure 4: Box diagrams contributing to the decay $b \rightarrow q\nu\bar{\nu}$, $q = d, s$, at $O(\alpha_s)$. The curly and double lines represent gluons and quarks (or squarks), respectively. The remaining internal lines denote gauge bosons, leptons, charged Higgs bosons, scalar leptons and charginos. The diagrams for $b \rightarrow ql^+l^-$ can be obtained by the replacements $l \leftrightarrow \nu$ and $\tilde{l} \rightarrow \tilde{\nu}$. The symmetric diagrams are not shown here explicitly.

$$[B_R^{\nu\bar{\nu}}]_{\tilde{\chi}} = -\kappa_q s_W^2 \sum_{i,j=1}^2 \sum_{a,b=1}^6 \frac{\sqrt{x_{ji}}}{M_{\tilde{\chi}_i}^2} (X_j^{E_L})_{bf} (X_i^{E_L\dagger})_{fb} (X_j^{U_R\dagger})_{qa} (X_i^{U_R})_{a3} \left\{ f_6^{(0)}(x_{ji}, y_{ai}, z_{bi}) + \frac{\alpha_s}{4\pi} \left[f_9^{(1)}(x_{ji}, y_{ai}, z_{bi}) + 4 \left(1 + y_{ai} \frac{\partial}{\partial y_{ai}} \right) f_6^{(0)}(x_{ji}, y_{ai}, z_{bi}) L_{\tilde{u}_a} \right] \right\}, \quad (3.24)$$

$$[B_L^{\nu\bar{\nu}}]_4 = -\frac{\alpha_s}{4\pi} \frac{\kappa_q s_W^2}{3} \sum_{i,j=1}^2 \sum_{a,\dots,d=1}^6 \frac{1}{M_{\tilde{\chi}_i}^2} (X_j^{E_L})_{cf} (X_i^{E_L\dagger})_{fc} (X_j^{U_L\dagger})_{qb} (X_i^{U_L})_{a3} \times [(P_U)_{ad} y_{di} (P_U)_{db} (1 + L_{\tilde{u}_d})] f_9^{(0)}(x_{ji}, y_{ai}, y_{bi}, z_{ci}), \quad (3.25)$$

$$[B_R^{\nu\bar{\nu}}]_4 = \frac{\alpha_s}{4\pi} \frac{2\kappa_q s_W^2}{3} \sum_{i,j=1}^2 \sum_{a,\dots,d=1}^6 \frac{\sqrt{x_{ji}}}{M_{\tilde{\chi}_i}^2} (X_j^{E_L})_{cf} (X_i^{E_L\dagger})_{fc} (X_j^{U_R\dagger})_{qb} (X_i^{U_R})_{a3} \times [(P_U)_{ad} y_{di} (P_U)_{db} (1 + L_{\tilde{u}_d})] f_{10}^{(0)}(x_{ji}, y_{ai}, y_{bi}, z_{ci}), \quad (3.26)$$

where, as before, $f = e, \mu, \tau$ and $q = 1 (2)$ for the $b \rightarrow d$ ($b \rightarrow s$) transition.

3.3 The $b \rightarrow s(d)l^+l^-$ transition

The part of the effective Hamiltonian describing the transition $b \rightarrow ql^+l^-$ ($q = d, s$) that is relevant for the decay $\bar{B}_q \rightarrow l^+l^-$ has the form

$$\mathcal{H}_{\text{eff}} = -\frac{2G_F}{\sqrt{2}} \frac{\alpha}{2\pi \sin^2 \theta_W} V_{tb} V_{tq}^* [c_A \mathcal{O}_A + c'_A \mathcal{O}'_A + c_S \mathcal{O}_S + c'_S \mathcal{O}'_S + c_P \mathcal{O}_P + c'_P \mathcal{O}'_P], \quad (3.27)$$

where

$$\mathcal{O}_A = (\bar{q}\gamma^\mu P_L b)(\bar{l}\gamma_\mu\gamma_5 l), \quad \mathcal{O}'_A = (\bar{q}\gamma^\mu P_R b)(\bar{l}\gamma_\mu\gamma_5 l), \quad (3.28)$$

$$\mathcal{O}_S = m_b(\bar{q}P_R b)(\bar{l}l), \quad \mathcal{O}'_S = m_q(\bar{q}P_L b)(\bar{l}l), \quad (3.29)$$

$$\mathcal{O}_P = m_b(\bar{q}P_R b)(\bar{l}\gamma_5 l), \quad \mathcal{O}'_P = m_q(\bar{q}P_L b)(\bar{l}\gamma_5 l). \quad (3.30)$$

Again, the effective Hamiltonian [Eq. (3.27)] has been obtained by exploiting the Glashow-Iliopoulos-Maiani (GIM) mechanism [34], as discussed in Sec. 3.2.

As far as additional operators like $(\bar{q}\gamma^\mu P_{L,R} b)(\bar{l}\gamma_\mu l)$ and $(\bar{q}\sigma^{\mu\nu} P_{L,R} b)(\bar{l}\sigma_{\mu\nu} P_{L,R} l)$ are concerned, they also receive contributions within SUSY. However, as we shall see in Sec. 5.1.2, the hadronic matrix elements of these vector and tensor operators vanish. Moreover, the corresponding Wilson coefficients do not mix with the remaining short-distance coefficients.

The Wilson coefficients can then be written as

$$c_A = \sum_{J=\text{SM}, H, \tilde{\chi}, 4} \{[C_A^{l\bar{l}}]_J + [B_A^{l\bar{l}}]_J\}, \quad c'_A = \sum_{J=\text{SM}, H, \tilde{\chi}, 4} \{[C_{A'}^{l\bar{l}}]_J + [B_{A'}^{l\bar{l}}]_J\}, \quad (3.31a)$$

$$c_S = \sum_{J=H, \tilde{\chi}, 4} \{[N_S^{l\bar{l}}]_J + [B_S^{l\bar{l}}]_J\}, \quad c'_S = \sum_{J=H, \tilde{\chi}, 4} \{[N_{S'}^{l\bar{l}}]_J + [B_{S'}^{l\bar{l}}]_J\}, \quad (3.31b)$$

$$c_P = \sum_{J=H, \tilde{\chi}, 4} \{[N_P^{l\bar{l}}]_J + [B_P^{l\bar{l}}]_J\}, \quad c'_P = \sum_{J=H, \tilde{\chi}, 4} \{[N_{P'}^{l\bar{l}}]_J + [B_{P'}^{l\bar{l}}]_J\}. \quad (3.31c)$$

There are several points to be made here. (a) The SM contribution to scalar and pseudoscalar operators is suppressed by $m_l m_{b,q} / M_W^2$, and so can be neglected. (b) The Z^0 boson as a vector particle does not contribute to scalar and pseudoscalar operators. (c) Because of their scalar-type couplings, the neutral Higgs bosons do not contribute to the Wilson coefficients c_A and c'_A .

3.3.1 Z^0 -penguin contributions

Evaluation of the diagrams with Z^0 exchange results in

$$[C_A^{l\bar{l}}]_J = -[C_L^{\nu\bar{\nu}}]_J, \quad [C_{A'}^{l\bar{l}}]_J = -[C_R^{\nu\bar{\nu}}]_J \quad (J = \text{SM}, H, \tilde{\chi}, 4), \quad (3.32)$$

with the functions $[C_L^{\nu\bar{\nu}}]_J$ and $[C_R^{\nu\bar{\nu}}]_J$ as given in Eqs. (3.10)–(3.17).

3.3.2 Box-diagram contributions

$$[B_A^{l\bar{l}}]_{\text{SM}} = \frac{1}{4} \left\{ f_2^{(0)}(x) + \frac{\alpha_s}{4\pi} \left[f_7^{(1)}(x) + 8x \frac{\partial}{\partial x} f_2^{(0)}(x) L_t \right] \right\}, \quad (3.33)$$

$$[B_{A'}^{l\bar{l}}]_{\text{SM}} = 0, \quad (3.34)$$

$$[B_{S,P}^{l\bar{l}}]_{\text{SM}} = [B_{S',P'}^{l\bar{l}}]_{\text{SM}} = 0, \quad (3.35)$$

$$[B_A^{l\bar{l}}]_H = 0, \quad (3.36)$$

$$[B_{A'}^{l\bar{l}}]_H = -\frac{m_b m_q m_l^2 \tan^4 \beta}{16 M_W^2 M_H^2} \left\{ f_2^{(0)}(y) + \frac{\alpha_s}{4\pi} \left[f_7^{(1)}(y) + 8 \left(1 + y \frac{\partial}{\partial y} \right) f_2^{(0)}(y) L_t \right] \right\}, \quad (3.37)$$

$$[B_{S,P}^{l\bar{l}}]_H = \pm \frac{m_l \tan^2 \beta}{4 M_W^2} \left\{ f_7^{(0)}(x, z) + \frac{\alpha_s}{4\pi} \left[f_{11}^{(1)}(x, z) + 8x \frac{\partial}{\partial x} f_7^{(0)}(x, z) L_t \right] \right\}, \quad (3.38)$$

$$[B_{S',P'}^{l\bar{l}}]_H = \frac{m_l \tan^2 \beta}{4 M_W^2} \left\{ f_7^{(0)}(x, z) + \frac{\alpha_s}{4\pi} \left[f_{11}^{(1)}(x, z) + 8x \frac{\partial}{\partial x} f_7^{(0)}(x, z) L_t \right] \right\}, \quad (3.39)$$

$$\begin{aligned} [B_A^{l\bar{l}}]_{\tilde{\chi}} &= \kappa_q s_W^2 \sum_{i,j=1}^2 \sum_{f=1}^3 \sum_{a=1}^6 \frac{(X_j^{U_L\dagger})_{qa} (X_i^{U_L})_{a3}}{M_{\tilde{\chi}_i}^2} \left\{ \frac{1}{2} \left\{ f_5^{(0)}(x_{ji}, y_{ai}, v_{fi}) \right. \right. \\ &+ \frac{\alpha_s}{4\pi} \left[f_8^{(1)}(x_{ji}, y_{ai}, v_{fi}) + 4 \left(1 + y_{ai} \frac{\partial}{\partial y_{ai}} \right) f_5^{(0)}(x_{ji}, y_{ai}, v_{fi}) L_{\tilde{u}_a} \right] \left. \right\} (X_i^{N_L\dagger})_{lf} (X_j^{N_L})_{fl} \\ &+ \sqrt{x_{ji}} \left\{ f_6^{(0)}(x_{ji}, y_{ai}, v_{fi}) + \frac{\alpha_s}{4\pi} \left[f_9^{(1)}(x_{ji}, y_{ai}, v_{fi}) + 4 \left(1 + y_{ai} \frac{\partial}{\partial y_{ai}} \right) f_6^{(0)}(x_{ji}, y_{ai}, v_{fi}) L_{\tilde{u}_a} \right] \right\} \\ &\times (X_i^{N_R\dagger})_{lf} (X_j^{N_R})_{fl} \left. \right\}, \end{aligned} \quad (3.40)$$

$$[B_{A'}^{l\bar{l}}]_{\tilde{\chi}} = -[B_A^{l\bar{l}}]_{\tilde{\chi}} (X^{U_L} \rightarrow X^{U_R}; X^{N_L} \leftrightarrow X^{N_R}), \quad (3.41)$$

$$\begin{aligned} [B_{S,P}^{l\bar{l}}]_{\tilde{\chi}} &= \pm \frac{\kappa_q s_W^2}{m_b} \sum_{i,j=1}^2 \sum_{f=1}^3 \sum_{a=1}^6 \frac{(X_j^{U_L\dagger})_{qa} (X_i^{U_R})_{a3}}{M_{\tilde{\chi}_i}^2} \left\{ \left\{ f_5^{(0)}(x_{ji}, y_{ai}, v_{fi}) \right. \right. \\ &+ \frac{\alpha_s}{4\pi} \left[f_{12}^{(1)}(x_{ji}, y_{ai}, v_{fi}) + 4y_{ai} \frac{\partial}{\partial y_{ai}} f_5^{(0)}(x_{ji}, y_{ai}, v_{fi}) L_{\tilde{u}_a} \right] \left. \right\} (X_i^{N_R\dagger})_{lf} (X_j^{N_L})_{fl} \\ &\pm \sqrt{x_{ji}} \left\{ f_6^{(0)}(x_{ji}, y_{ai}, v_{fi}) + \frac{\alpha_s}{4\pi} \left[f_{13}^{(1)}(x_{ji}, y_{ai}, v_{fi}) + 4y_{ai} \frac{\partial}{\partial y_{ai}} f_6^{(0)}(x_{ji}, y_{ai}, v_{fi}) L_{\tilde{u}_a} \right] \right\} \\ &\times (X_i^{N_L\dagger})_{lf} (X_j^{N_R})_{fl} \left. \right\}, \end{aligned} \quad (3.42)$$

$$[B_{S',P'}^{l\bar{l}}]_{\tilde{\chi}} = \pm [B_{S,P}^{l\bar{l}}]_{\tilde{\chi}} (X^{U_L} \leftrightarrow X^{U_R}; X^{N_L} \leftrightarrow X^{N_R}; m_b \rightarrow m_q). \quad (3.43)$$

Here l denotes the external leptons (not summed over) and f labels the flavour of the intermediate neutrino and its scalar partner. The loop functions $f_p^{(0)}, f_{p'}^{(1)}$ are given in Appendix B.

Turning to the contributions from the quartic couplings, we obtain

$$\begin{aligned} [B_A^{l\bar{l}}]_4 &= -\frac{\alpha_s}{4\pi} \frac{2\kappa_q s_W^2}{3} \sum_{i,j=1}^2 \sum_{f=1}^3 \sum_{a,b,c=1}^6 \frac{(X_j^{U_L\dagger})_{qb}(X_i^{U_L})_{a3}}{M_{\tilde{\chi}_i}^2} [(P_U)_{ac} y_{ci} (P_U)_{cb} (1 + L_{\tilde{u}_c})] \\ &\times \left\{ \frac{1}{2} f_9^{(0)}(x_{ji}, y_{ai}, y_{bi}, v_{fi}) (X_i^{N_L\dagger})_{lf} (X_j^{N_L})_{fl} + \sqrt{x_{ji}} f_{10}^{(0)}(x_{ji}, y_{ai}, y_{bi}, v_{fi}) (X_i^{N_R\dagger})_{lf} (X_j^{N_R})_{fl} \right\}, \end{aligned} \quad (3.44)$$

$$[B_{A'}^{l\bar{l}}]_4 = -[B_A^{l\bar{l}}]_4 (X^{U_L} \rightarrow X^{U_R}; X^{N_L} \leftrightarrow X^{N_R}), \quad (3.45)$$

$$\begin{aligned} [B_{S,P}^{l\bar{l}}]_4 &= \mp \frac{\alpha_s}{4\pi} \frac{2\kappa_q s_W^2}{3m_b} \sum_{i,j=1}^2 \sum_{f=1}^3 \sum_{a,b,c=1}^6 \frac{(X_j^{U_L\dagger})_{qb}(X_i^{U_R})_{a3}}{M_{\tilde{\chi}_i}^2} [(P_U)_{ac} y_{ci} (P_U)_{cb} (1 + L_{\tilde{u}_c})] \\ &\times \left\{ f_9^{(0)}(x_{ji}, y_{ai}, y_{bi}, v_{fi}) (X_i^{N_R\dagger})_{lf} (X_j^{N_L})_{fl} \pm \sqrt{x_{ji}} f_{10}^{(0)}(x_{ji}, y_{ai}, y_{bi}, v_{fi}) (X_i^{N_L\dagger})_{lf} (X_j^{N_R})_{fl} \right\}, \end{aligned} \quad (3.46)$$

$$[B_{S',P'}^{l\bar{l}}]_4 = \pm [B_{S,P}^{l\bar{l}}]_4 (X^{U_L} \leftrightarrow X^{U_R}; X^{N_L} \leftrightarrow X^{N_R}; m_b \rightarrow m_q). \quad (3.47)$$

3.3.3 Neutral Higgs boson penguin diagrams

As we have already mentioned, the contributions of neutral Higgs bosons are relevant only for large values of $\tan \beta$. In this case, we obtain

$$[N_{S,P}^{l\bar{l}}]_H = \mp \frac{m_l \tan^2 \beta}{4M_W^2} \left\{ x f_3^{(0)}(x, z) + \frac{\alpha_s}{4\pi} \left[f_{14}^{(1)}(x, z) + 8x \frac{\partial}{\partial x} [x f_3^{(0)}(x, z)] L_t \right] \right\}, \quad (3.48)$$

$$[N_{S',P'}^{l\bar{l}}]_H = \pm [N_{S,P}^{l\bar{l}}]_H^*, \quad (3.49)$$

$$\begin{aligned} [N_{S,P}^{l\bar{l}}]_{\tilde{\chi}} &= \pm \frac{m_l \tan^2 \beta}{M_W(M_H^2 - M_W^2)} \sum_{i,j=1}^2 \sum_{a,b=1}^6 \sum_{m,n=1}^3 \Gamma_{imn}^a (\Gamma_{bm}^{U_L})_{bm} U_{j2} a_Y \\ &\times \left[a_0 + a_1 \tan \beta + \frac{\alpha_s}{4\pi} a_2 m_q^2 \tan^2 \beta \right], \end{aligned} \quad (3.50)$$

$$[N_{S',P'}^{l\bar{l}}]_{\tilde{\chi}} = \pm [N_{S,P}^{l\bar{l}}]_{\tilde{\chi}}^* (m_q \rightarrow m_b, \lambda_{mn}^* \rightarrow \lambda_{nm}), \quad (3.51)$$

where

$$\Gamma_{imn}^a \equiv \frac{1}{2\sqrt{2}} [\sqrt{2}M_W V_{i1}(\Gamma^{U_L\dagger})_{na} a_g - (M_U)_{nn} V_{i2}(\Gamma^{U_R\dagger})_{na} a_Y] \lambda_{mn}, \quad (3.52)$$

$$\lambda_{mn} \equiv \frac{V_{mb} V_{nq}^*}{V_{tb} V_{tq}^*}, \quad (3.53)$$

with a_g, a_Y defined in Eq. (2.22). The coefficients a_0, a_1, a_2 in Eq. (3.50) are given by

$$\begin{aligned} a_0 &= \mp \left[\sqrt{x_{ij}} \left\{ f_3^{(0)}(x_{ij}, y_{aj}) + \frac{\alpha_s}{4\pi} \left[f_{18}^{(1)}(x_{ij}, y_{aj}) + 4y_{ai} \frac{\partial}{\partial y_{ai}} f_3^{(0)}(x_{ij}, y_{aj}) L_{\tilde{u}_a} \right] \right\} U_{i2} V_{j1} \right. \\ &\quad \pm \left. \left\{ f_4^{(0)}(x_{ij}, y_{aj}) + \frac{\alpha_s}{4\pi} \left[f_{19}^{(1)}(x_{ij}, y_{aj}) + 4y_{ai} \frac{\partial}{\partial y_{ai}} f_4^{(0)}(x_{ij}, y_{aj}) L_{\tilde{u}_a} \right] \right\} U_{j2}^* V_{i1}^* \right] \delta_{ab} \\ &\quad + \frac{(\Delta_i^\pm)_{ab}}{M_W} \left\{ f_3^{(0)}(y_{ai}, y_{bi}) + \frac{\alpha_s}{4\pi} \left[f_{17}^{(1)}(y_{ai}, y_{bi}) + 4 \left(1 + y_{ai} \frac{\partial}{\partial y_{ai}} + y_{bi} \frac{\partial}{\partial y_{bi}} \right) f_3^{(0)}(y_{ai}, y_{bi}) L_{\tilde{u}_a} \right] \right\} \delta_{ij} \\ &\quad + \frac{\alpha_s}{4\pi} \left[\frac{4\Gamma_{imn}^{a*}}{M_W (\Gamma^{U_L})_{bm} \lambda_{mn}^* U_{j2}} \right] f_{15}^{(1)}(y_{ai}) \delta_{ij} \delta_{ab} \delta_{mn}, \end{aligned} \quad (3.54)$$

$$a_1 = \frac{M_{\tilde{\chi}_i}}{\sqrt{2}M_W} \left\{ f_8^{(0)}(y_{ai}) + \frac{\alpha_s}{4\pi} \left[f_{16}^{(1)}(y_{ai}) + 4y_{ai} \frac{\partial}{\partial y_{ai}} f_8^{(0)}(y_{ai}) L_{\tilde{u}_a} \right] \right\} \delta_{ij} \delta_{ab}, \quad (3.55)$$

$$a_2 = \frac{(\Gamma^{U_L\dagger})_{mb} \lambda_{mn} U_{j2}^*}{2M_W \Gamma_{imn}^a} f_{15}^{(1)}(y_{ai}) \delta_{ij} \delta_{ab} \delta_{mn}, \quad (3.56)$$

with

$$(\Delta_i^\pm)_{ab} \equiv \sum_{f=1}^3 \frac{(M_U)_{ff}}{\sqrt{2}M_{\tilde{\chi}_i}} [\mu^* (\Gamma^{U_R})_{af} (\Gamma^{U_L\dagger})_{fb} \pm \mu (\Gamma^{U_L})_{af} (\Gamma^{U_R\dagger})_{fb}]. \quad (3.57)$$

It is interesting to note that the contribution in Eqs. (3.50) and (3.51) that is proportional to $a_1 \tan^3 \beta$ comes from the counterterm of the electroweak wave function renormalization. Since it is not suppressed by the mass of the light quarks, it gives by far the dominant contribution in the high $\tan \beta$ regime. (Further details may be found in Ref. [26].)

Finally, the calculation of the diagrams involving quartic squark couplings yields

$$\begin{aligned} [N_{S,P}^{l\bar{l}}]_4 &= \mp \frac{\alpha_s}{4\pi} \frac{2m_l \tan^2 \beta}{3M_W^2 (M_H^2 - M_W^2)} \sum_{i,j=1}^2 \sum_{m,n=1}^3 \sum_{a,\dots,e,g,k=1}^6 \Gamma_{imn}^a (\Gamma^{U_L})_{dm} U_{j2} a_Y \\ &\quad \times \left\{ (P_U)_{ek} y_{kj} (P_U)_{kg} (1 + L_{\tilde{u}_k}) \left\{ \tan \beta \frac{M_{\tilde{\chi}_i}}{\sqrt{2}} f_3^{(0)}(y_{ai}, y_{di}) \delta_{ij} \delta_{ae} \delta_{gd} \right. \right. \\ &\quad + (\Delta_i^\pm)_{bc} \left[\delta_{ae} \delta_{gb} \delta_{cd} f_6^{(0)}(y_{ai}, y_{bi}, y_{ci}) + \delta_{ab} \delta_{ce} \delta_{gd} f_6^{(0)}(y_{ai}, y_{ci}, y_{di}) \right] \delta_{ij} \\ &\quad \mp M_W \left[\sqrt{x_{ij}} f_6^{(0)}(x_{ij}, y_{aj}, y_{dj}) U_{i2} V_{j1} \pm f_5^{(0)}(x_{ij}, y_{aj}, y_{dj}) U_{j2}^* V_{i1}^* \right] \delta_{ae} \delta_{dg} \left. \right\} \\ &\quad - (P_U)_{ae} [1 + L_{\tilde{u}_g} - f_{11}^{(0)}(y_{ej}, y_{gj})] (P_U)_{gd} (\Delta_i^\pm)_{eg} \delta_{ij} f_3^{(0)}(y_{ai}, y_{di}) \left. \right\}, \end{aligned} \quad (3.58)$$

$$[N_{S',P'}^{l\bar{l}}]_4 = \pm [N_{S,P}^{l\bar{l}}]_4^*(\lambda_{mn}^* \rightarrow \lambda_{nm}). \quad (3.59)$$

Notice that there is again a $\tan^3 \beta$ enhancement in Eqs. (3.58) and (3.59), due to the counterterm contributions.

3.4 The $\bar{s} \rightarrow \bar{d}\nu\bar{\nu}$ transition

The results for the $\bar{s} \rightarrow \bar{d}\nu\bar{\nu}$ transition related to the coupling $V_{ts}^*V_{td}$ can easily be obtained from the results of Sec. 3.2 through the appropriate replacements of flavours. However, unlike the $b \rightarrow s(d)\nu\bar{\nu}$ transition, the internal charm-quark contribution to $\bar{s} \rightarrow \bar{d}\nu\bar{\nu}$ cannot be neglected, since $|V_{cs}^*V_{cd}|/|V_{ts}^*V_{td}| \sim 70$, which partially compensates for the suppression of the charm-quark relative to the top-quark contributions due to $m_c^2 \ll m_t^2$ [cf. Eq. (3.5)]. Yet, it turns out that the new-physics contributions proportional to $V_{cs}^*V_{cd}$ are small. Accordingly, the charm contribution is completely described by the SM for which next-to-leading-order corrections are known from [12, 13].

The effective Hamiltonian may then be written as

$$\mathcal{H}_{\text{eff}} = \frac{4G_F}{\sqrt{2}} \frac{\alpha}{2\pi \sin^2 \theta_W} \sum_f [V_{cs}^*V_{cd} X_{\text{NL}}^f \mathcal{O}_L + V_{ts}^*V_{td} (c_L \mathcal{O}_L + c_R \mathcal{O}_R)], \quad (3.60)$$

where $f = e, \mu, \tau$ and

$$\mathcal{O}_L = (\bar{s}\gamma_\mu P_L d)(\bar{\nu}_f \gamma^\mu P_L \nu_f), \quad \mathcal{O}_R = (\bar{s}\gamma_\mu P_R d)(\bar{\nu}_f \gamma^\mu P_R \nu_f). \quad (3.61)$$

The coefficients c_L and c_R are given by Eqs. (3.9)–(3.26) if we make the replacements

$$m_b m_q \rightarrow m_d m_s, \quad \kappa_q \rightarrow \bar{\kappa} = \frac{1}{8\sqrt{2}G_F e^2 V_{td} V_{ts}^*}. \quad (3.62)$$

Additionally, the indices of the matrices $X_i^{U_{L,R}}$ in Eqs. (3.14)–(3.17) and (3.23)–(3.26) should be changed as follows: $q \rightarrow 2, 3 \rightarrow 1$. Note that the results of the previous subsections suggest that the contributions of the Wilson coefficient c_R can be neglected in the case of the $s \rightarrow d$ transition. Indeed, since c_R involves always the factors $m_s m_d / M_W^2$, it is far too small to give an appreciable contribution.

As for the function X_{NL}^f in Eq. (3.60), it results from the next-to-leading order calculation [13], and is given explicitly in Ref. [12], where numerical values of X_{NL}^f for $\mu = m_c$ and different choices of $\Lambda_{\text{MS}}^{(4)}$ and m_c may be found. Note that there is typically a 30% suppression of the charm contribution due to the QCD corrections.

3.5 The $\bar{s} \rightarrow \bar{d}l^+l^-$ transition

The results for this transition can be readily obtained from those given in Sec. 3.3. As in the $\bar{s} \rightarrow \bar{d}\nu\bar{\nu}$ transition, the charm contribution proportional to $V_{cs}^*V_{cd}$ cannot be neglected. However, it turns out that the new-physics effects in the charm sector are numerically small, and thus the charm contribution is dominated by that of the SM.

The effective Hamiltonian is then given by

$$\mathcal{H}_{\text{eff}} = -\frac{2G_F}{\sqrt{2}}\frac{\alpha}{2\pi \sin^2 \theta_W} \left[V_{cs}^*V_{cd}Y_{\text{NL}}\mathcal{O}_A + V_{ts}^*V_{td}(c_A\mathcal{O}_A + c'_A\mathcal{O}'_A + c_S\mathcal{O}_S + c'_S\mathcal{O}'_S + c_P\mathcal{O}_P + c'_P\mathcal{O}'_P) \right], \quad (3.63)$$

where the function Y_{NL} (the analogue of X_{NL}^f) has been calculated in Refs. [12, 13]. The remaining short-distance coefficients are given in Eqs. (3.31) with the replacements (3.62), together with

$$\lambda_{mn} \rightarrow \bar{\lambda}_{mn} \equiv \frac{V_{md}V_{ns}^*}{V_{td}V_{ts}^*}, \quad (3.64)$$

while the operators can be obtained from Eqs. (3.28)–(3.30) through the appropriate changes of flavours.

3.6 Renormalization group evolution and scale dependence

The renormalization scale dependence of the Wilson coefficients $\vec{C}(\mu)$ is governed by

$$\frac{d}{d \ln \mu} \vec{C}(\mu) = \hat{\gamma}^T \vec{C}(\mu), \quad (3.65)$$

where $\hat{\gamma}$ is the anomalous dimension matrix.⁶ Since the anomalous dimensions for all operators in Eqs. (3.8), (3.28)–(3.30) and (3.61) vanish, the Wilson coefficients must be independent of μ . Otherwise the physical amplitudes would depend on the renormalization scale.

We now demonstrate that all contributions from the Z^0 -penguin diagrams, as well as from box and penguin diagrams with neutral Higgs bosons, are separately independent of μ when $\mathcal{O}(\alpha_s)$ corrections are taken into account.

In the leading-order expressions of the Wilson coefficients, there are two sources of scale dependence. Firstly, the running quark mass

$$m_q(\mu) = m_q(\mu_0) \left[\frac{\alpha_s(\mu)}{\alpha_s(\mu_0)} \right]^{\gamma_m^{(0)}/(2\beta_0)}, \quad \gamma_m^{(0)} = 8, \quad \beta_0 = 11 - \frac{2}{3}n_f, \quad (3.66)$$

⁶For a detailed discussion see, e.g., Refs. [35, 36].

where $m_q(\mu_0)$ is the value of the quark mass at the scale μ_0 and n_f is the number of active flavours. To first order in α_s , the above expression can be written as

$$m_q(\mu) = m_q(\mu_0) \left[1 - \frac{\gamma_m^{(0)}}{2} \frac{\alpha_s(\mu_0)}{4\pi} \ln \left(\frac{\mu^2}{\mu_0^2} \right) \right]. \quad (3.67)$$

Secondly, the running squark mass

$$m_{\tilde{q}}(\mu) = m_{\tilde{q}}(\mu_0) \left[\frac{\alpha_s(\mu)}{\alpha_s(\mu_0)} \right]^{\gamma_{\tilde{m}}^{(0)}/(2\beta_0)}, \quad \gamma_{\tilde{m}}^{(0)} = 4, \quad (3.68)$$

which to first order in α_s can be written as

$$m_{\tilde{q}}(\mu) = m_{\tilde{q}}(\mu_0) \left[1 - \frac{\gamma_{\tilde{m}}^{(0)}}{2} \frac{\alpha_s(\mu_0)}{4\pi} \ln \left(\frac{\mu^2}{\mu_0^2} \right) \right]. \quad (3.69)$$

The μ dependence of the top-quark mass in the leading-order terms in both the SM and the 2HDM coefficients is cancelled by the α_s corrections of the Wilson coefficients that involve the derivatives of the leading functions [see, e.g., Eqs. (3.10) and (3.12)]. The same applies to the μ dependence of the squark masses in the supersymmetric contributions [see, e.g., Eq. (3.14)].

As can be seen, for example, from Eq. (3.13), there is an additional μ dependence in the leading contributions of the new operators generated by charged Higgs-boson exchanges that is related to the light quark masses present in the Yukawa couplings. This dependence on μ is cancelled by the $O(\alpha_s)$ corrections proportional to the leading functions.

Finally, we observe that in the chargino sector there are additional μ dependencies in the chargino-squark-quark vertices, which are given in Eqs. (2.17) and (2.18). These μ dependencies arise not only from the μ dependence of M_U and M_D but also from the coefficients a_g and a_Y given in Eq. (2.22). Taking into account both μ dependencies, the effective μ dependence of the vertex $X_i^{U_{L,R}}$ is given by

$$X_i^{U_{L,R}}(\mu) = X_i^{U_{L,R}}(M_{\tilde{g}}) \left[1 - 2 \frac{\alpha_s(\mu)}{4\pi} \ln \left(\frac{\mu^2}{M_{\tilde{g}}^2} \right) \right]. \quad (3.70)$$

This μ dependence is cancelled by the corresponding dependence in the $O(\alpha_s)$ corrections proportional to the leading functions [see, e.g., Eq. (3.14)]. We observe that the μ dependence of a_g and a_Y is essential to obtain μ -independent chargino contributions. The μ dependence in a_g and a_Y is related to the fact that the effective theory does not contain gluinos, which have been integrated out at the scale $O(M_{\tilde{g}})$. Thus, in the effective theory the gaugino and Higgsino couplings renormalize differently from the ordinary gauge and Yukawa couplings. If one expresses the supersymmetric couplings at $\mu \ll M_{\tilde{g}}$ in terms of the SM couplings such as g and the top Yukawa coupling, this difference has to be taken into account in order to obtain correct results.

An additional μ dependence arises in the MSSM from the $O(\alpha_s)$ contributions due to the quartic squark vertex. Note that only the μ dependence from gluonic corrections has been taken into account

in Eqs. (3.68) and (3.69). The inclusion of the contribution from the quartic squark coupling results in a modification of the anomalous dimension $\gamma_{\tilde{m}}^{(0)}$. This additional contribution would then cancel the μ dependence present in the two-loop diagrams with quartic squark couplings denoted by the subscript $J = 4$ in Eqs. (3.9) and (3.31). In the next section, we will give a recipe how to avoid the appearance of the quartic squark coupling using an on-shell prescription for the squark mass. In this sense Eqs. (3.68) and (3.69) can be considered as complete.

4 Details of the calculation

In this section we present the details of the calculation. Readers who are not interested in these technical issues should proceed to Sec. 5.

For processes that take place at scales much lower than M_W , models such as the SM, 2HDM and MSSM can be replaced by an effective theory by means of integrating out all particles heavier than $O(M_W)$. Our aim is to find the QCD corrections to the Wilson coefficients of the relevant operators in the effective theory. The operators of interest are given in Eqs. (3.8) and (3.28)–(3.30) for the quark-level transition $b \rightarrow s(d)\nu\bar{\nu}$ and $b \rightarrow s(d)l^+l^-$, respectively. (The presentation given below applies to $b \rightarrow sl^+l^-$ transitions and with obvious changes to $b \rightarrow s\nu\bar{\nu}$.)

The simplest way of finding the Wilson coefficients is to require equality of one-particle-irreducible (1PI) amputated Green's functions calculated in the full and effective theory. The former requires the calculation of box- and penguin-type diagrams. The different possible topologies can be found in Figs. 1–4. Note that photonic penguin diagrams do not contribute to the processes under consideration. Within the SM, the neutral Higgs boson penguin contributions are negligibly small, since they are suppressed by the light lepton and quark masses and not enhanced by $\tan\beta$. All together we have 16 box diagrams in the SM, additional 20 box diagrams in the 2HDM and 4 box diagrams in the chargino sector of the MSSM. Further, the number of Z^0 -penguin diagrams amounts to 40 in the SM, additional 16 in the 2HDM and 20 in the chargino sector. Note that the topology shown in Fig. 2 is present only in the chargino sector. We have 240 diagrams containing neutral Higgs bosons in the 2HDM and 64 neutral Higgs penguin diagrams containing charginos and squarks. While counting the diagrams, different quark and squark flavours, as well as different chargino generations, are not taken into account. Note that the up- and charm-quark contributions to the SM and 2HDM Wilson coefficients are included via the GIM mechanism, as explained in Sec. 3.2. The sum over all squarks and charginos is shown explicitly in our results.

The calculation has been performed within a covariant R_{ξ_g} and R_{ξ_W} gauge for the gluon and the W boson, respectively, which provides a useful check of our computation. The contributions of the penguin and box diagrams to the Wilson coefficients are separately *gauge independent* with respect to the gluon gauge, but in general *gauge dependent* with respect to the W -boson gauge. Thus, the

results presented in the previous sections are given in the 't Hooft-Feynman gauge for the W boson. We have checked that the sum of penguin and box diagrams contributing to the Wilson coefficients is independent of ξ_W .

We are interested in dimension six four-fermion operators, so the external momenta can be set to zero from the very beginning. The masses of the light quarks can be safely neglected as long as they are not enhanced by $\tan\beta$. That is, we neglect m_b , $m_{d,s}$ and m_l in the propagator, but keep them in the Yukawa couplings when multiplied by a factor of $\tan\beta$. Since we are interested in on-shell results, it is pertinent to ask whether we are allowed to keep light masses in the Yukawa coupling while neglecting external momenta. In fact, higher-order terms in external momenta would enlarge our operator basis, but also give contributions to Wilson coefficients of dimension-six operators after applying the equation of motion. However, these terms are not enhanced by $\tan\beta$ as they come solely from an expansion of the propagators, and therefore are negligible.

Setting the light quark masses to zero in the propagator produces infrared (IR) divergencies. We regularize the IR and ultraviolet (UV) divergencies simultaneously in $D = 4 - 2\varepsilon$ dimensions. At one-loop level, the UV divergencies in the penguin diagrams can be removed by the electroweak renormalization of the wave function. We have chosen an on-shell prescription, following the approach of Ref. [26]. The QCD renormalization, which becomes necessary at the two-loop level, is performed in the $\overline{\text{MS}}$ scheme.

As mentioned earlier, the results for the Wilson coefficients presented in Sec. 3 are given in terms of the running $\overline{\text{MS}}$ quark and squark masses $m_q \equiv m_q(\mu)$ and $m_{\tilde{q}} \equiv m_{\tilde{q}}(\mu)$, respectively. Alternatively, one can work with the pole masses, in which case the following steps should be performed:

Step 1 Remove the contributions due to quartic squark couplings (i.e. the contributions with the index $J = 4$).

Step 2 Make a shift from the $\overline{\text{MS}}$ scheme to the corresponding pole masses, namely:⁷

$$m_t(\mu) = m_t^{\text{pole}} \left\{ 1 - \frac{\alpha_s(m_t^{\text{pole}})}{4\pi} \left[\frac{16}{3} - 4 \ln \left(\frac{m_t^{\text{pole}}}{\mu} \right)^2 \right] \right\}, \quad (4.1)$$

$$m_q(\mu) = m_q^{\text{pole}} \left[1 - \frac{\alpha_s(m_q^{\text{pole}})}{4\pi} \frac{16}{3} \right] \left[\frac{\alpha_s(\mu)}{\alpha_s(m_q^{\text{pole}})} \right]^{\gamma_m^{(0)}/(2\beta_0)} \times \left\{ 1 + \left[\frac{\gamma_m^{(1)}}{2\beta_0} - \frac{\beta_1 \gamma_m^{(0)}}{2\beta_0^2} \right] \frac{\alpha_s(\mu) - \alpha_s(m_q^{\text{pole}})}{4\pi} \right\} \quad (q = d, s, b), \quad (4.2)$$

$$m_{\tilde{q}}(\mu) = m_{\tilde{q}}^{\text{pole}} \left\{ 1 - \frac{\alpha_s(m_{\tilde{q}}^{\text{pole}})}{4\pi} \left[\frac{14}{3} - 2 \ln \left(\frac{m_{\tilde{q}}^{\text{pole}}}{\mu} \right)^2 \right] \right\}, \quad (4.3)$$

⁷Note that only in the case of light quarks (d, s, b) it is necessary to resum the large logarithms.

where

$$\gamma_m^{(1)} = \frac{404}{3} - \frac{40}{9}n_f, \quad \beta_1 = 102 - \frac{38}{3}n_f, \quad (4.4)$$

and $\gamma_m^{(0)}, \beta_0$ are given in Eq. (3.66). Observe that the shift in Eq. (4.3) involves only the gluonic corrections, since the contributions due to quartic squark couplings have already been considered in step 1. In this context, we would like to remark that the absence of the ‘quartic’ contributions in an on-shell scheme is related to the renormalization of the squark mass and mixing angle. (For details, we refer the reader to Ref. [37].)

After the proper renormalization, the left-over divergencies in the full and effective theory must be of infrared character, and they must cancel each other in the matching procedure. Note that in order to obtain this cancellation, the treatment of light masses must be identical in the full and the effective theory. As the light masses are zero, all unrenormalized loop diagrams in the effective theory vanish because of a cancellation of IR and UV divergencies, which considerably simplifies our calculation. The UV counterterms in the effective theory must therefore exactly reproduce the IR divergencies of the full theory, which provides a further check of the calculation. We wish to emphasize that owing to the dimensional regularization of the IR divergencies, the matching procedure must be performed in D dimensions [38].

In intermediate steps of the calculation structures like

$$(\gamma_{\alpha_1}\gamma_{\alpha_2}\gamma_{\alpha_3}P_A) \otimes (\gamma^{\alpha_1}\gamma^{\alpha_2}\gamma^{\alpha_3}P_B) \quad (4.5)$$

occur with $P_{A,B}$ being either P_L or P_R . They cannot be reduced using D dimensional Dirac algebra, due to the appearance of the matrix γ_5 . Only after the matching all divergencies cancel and the limit $D \rightarrow 4$ can be taken. Consequently, evanescent operators must be introduced in the effective theory. These operators appear in box diagrams in the SM and in the MSSM. For example, in the SM we define the evanescent operator for $b \rightarrow sl^+l^-$ as follows :

$$\mathcal{O}_1^E = (\bar{s}\gamma_{\alpha_1}\gamma_{\alpha_2}\gamma_{\alpha_3}P_L b)(\bar{l}\gamma^{\alpha_3}\gamma^{\alpha_2}\gamma^{\alpha_1}P_L l) - 4(\bar{s}\gamma_\mu P_L b)(\bar{l}\gamma^\mu P_L l). \quad (4.6)$$

(Further details can be found in [11].) In the chargino sector of the MSSM, operators with a different spinor ordering show up in box diagrams:

$$\tilde{\mathcal{O}}_{SAB} = (\bar{s}P_A l)(\bar{l}P_B b), \quad (4.7a)$$

$$\tilde{\mathcal{O}}_{VAB} = (\bar{s}\gamma_\alpha P_A l)(\bar{l}\gamma^\alpha P_B b), \quad (4.7b)$$

$$\tilde{\mathcal{O}}_{TAA} = (\bar{s}\sigma_{\alpha\beta} P_A l)(\bar{l}\sigma^{\alpha\beta} P_A b). \quad (4.7c)$$

We are not allowed to project these operators onto the operators given in Eqs. (3.28)–(3.30). For such a projection we would have to apply Fierz identities which cannot be continued to D dimensions. For

this reason, we have to define the following so-called ‘Fierz-vanishing’ evanescent operators [39,40]:

$$\tilde{\mathcal{O}}_{SLL}^E = \tilde{\mathcal{O}}_{SLL} + \frac{1}{2}\mathcal{O}_{SLL} - \frac{1}{8}\mathcal{O}_{TLL}, \quad (4.8a)$$

$$\tilde{\mathcal{O}}_{SLR}^E = \tilde{\mathcal{O}}_{SLR} + \frac{1}{2}\mathcal{O}_{VRL}, \quad (4.8b)$$

$$\tilde{\mathcal{O}}_{VLL}^E = \tilde{\mathcal{O}}_{VLL} - \mathcal{O}_{VLL}, \quad (4.8c)$$

$$\tilde{\mathcal{O}}_{VLR}^E = \tilde{\mathcal{O}}_{VLR} + 2\mathcal{O}_{SRL}, \quad (4.8d)$$

$$\tilde{\mathcal{O}}_{TLL}^E = \tilde{\mathcal{O}}_{TLL} - 6\mathcal{O}_{SLL} - \frac{1}{2}\mathcal{O}_{TLL}, \quad (4.8e)$$

as well as operators which can be obtained by an interchange of $P_L \leftrightarrow P_R$. The operators without tilde are identical to the ones given in Eqs. (4.7), but with exchanged l and b spinors. Moreover $\sigma_{\mu\nu} = [\gamma_\mu, \gamma_\nu]/2$. Due to a finite mixing into the physical operators the ‘Fierz-vanishing’ evanescent operators contribute at next-to-leading order. A similar situation was described in [11]. From Eq. (4.8e) it is evident that we cannot neglect the contributions to the tensor operator $\tilde{\mathcal{O}}_{TAA}$ as it affects the Wilson coefficients of the scalar operators. Furthermore the following evanescent operators are necessary at intermediate steps:

$$\begin{aligned} \tilde{\mathcal{O}}_1^E &= (\bar{s}\gamma_{\alpha_1}\gamma_{\alpha_2}\gamma_{\alpha_3}P_L l)(\bar{l}\gamma^{\alpha_1}\gamma^{\alpha_2}\gamma^{\alpha_3}P_L b) - 16\tilde{\mathcal{O}}_{VLL}, \\ \tilde{\mathcal{O}}_2^E &= (\bar{s}\gamma_{\alpha_1}\gamma_{\alpha_2}\gamma_{\alpha_3}P_L l)(\bar{l}\gamma^{\alpha_1}\gamma^{\alpha_2}\gamma^{\alpha_3}P_R b) - 4\tilde{\mathcal{O}}_{VLR}. \end{aligned} \quad (4.9)$$

5 Branching ratios

5.1 Rare B decays

5.1.1 $\bar{B} \rightarrow X_{d,s}\nu\bar{\nu}$

The decays $\bar{B} \rightarrow X_q\nu\bar{\nu}$ ($q = d, s$) are the cleanest theoretically in the field of rare B decays. Since the neutrinos escape detection, these decays are probed by requiring very large missing energy, $\hat{E}_q \equiv (E_B - E_{X_q})/m_b$ (for a full discussion see, e.g., Ref. [18]).

Using the effective Hamiltonian given in Eq. (3.7), we obtain the differential decay rate

$$\begin{aligned} \frac{d\mathcal{B}(\bar{B} \rightarrow X_q\nu\bar{\nu})}{d\hat{E}_q} &= \frac{4\alpha^2}{\pi^2 \sin^4 \theta_W} \frac{|V_{tb}V_{tq}^*|^2}{|V_{cb}|^2} \frac{\mathcal{B}(\bar{B} \rightarrow X_c e\bar{\nu}_e)\kappa(0)}{f(\hat{m}_c)\kappa(\hat{m}_c)} [(1 - \hat{E}_q)^2 - \hat{m}_q^2]^{1/2} \sum_f \\ &\times \left\{ (|c_L|^2 + |c_R|^2)[(1 - \hat{E}_q)(4\hat{E}_q - 1) + \hat{m}_q^2(1 - 3\hat{E}_q)] + 6\hat{m}_q(1 - 2\hat{E}_q - \hat{m}_q^2)\text{Re}(c_L^* c_R) \right\}, \end{aligned} \quad (5.1)$$

where the sum runs over the flavour of the three neutrinos, $\hat{m}_i \equiv m_i/m_b$, and the various input parameters are listed in Table 1. The expression for the missing energy spectrum is equivalent to the result presented in Ref. [18]. In writing Eq. (5.1), we have neglected non-perturbative corrections of $O(1/m_b^2)$ [43] and $O(1/m_c^2)$ [44, 45] which have been found to be small over most of the Dalitz plot.⁸ Furthermore, neglecting non-perturbative corrections, we have used the inclusive semileptonic decay rate

$$\Gamma(\bar{B} \rightarrow X_c e \bar{\nu}_e) = \frac{G_F^2 m_b^5}{192\pi^3} |V_{cb}|^2 f(\hat{m}_c) \kappa(\hat{m}_c) \quad (5.2)$$

in order to remove the uncertainties due to an overall factor of m_b^5 . The functions $f(\hat{m}_c)$ and $\kappa(\hat{m}_c)$ represent the phase-space and the one-loop QCD corrections, respectively [46]:

$$f(\hat{m}_c) = 1 - 8\hat{m}_c^2 + 8\hat{m}_c^6 - \hat{m}_c^8 - 24\hat{m}_c^4 \ln \hat{m}_c, \quad (5.3)$$

$$\kappa(\hat{m}_c) = 1 + \frac{\alpha_s(m_b)}{\pi} \frac{A_0(\hat{m}_c)}{f(\hat{m}_c)}, \quad (5.4)$$

where A_0 can be found in Ref. [47]. Expanding $\kappa(\hat{m}_c)$ in Eq. (5.4) around $\hat{m}_c = 0.3$ results in

$$\kappa(\hat{m}_c) \simeq 1 - \frac{\alpha_s(m_b)}{\pi} \left[1.670 + 2.027(0.3 - \hat{m}_c) + 2.152(0.3 - \hat{m}_c)^2 \right], \quad (5.5)$$

which is accurate to better than 1%, and hence perfectly adequate for our purposes. Further,

$$\kappa(0) = 1 + \frac{\alpha_s(m_b)}{\pi} \left[\frac{25}{6} - \frac{2}{3}\pi^2 \right] = 0.830 \quad (5.6)$$

represents the QCD correction to the matrix element of $b \rightarrow q\nu\bar{\nu}$ due to virtual and bremsstrahlung contributions [35].

Integration of Eq. (5.1) over $(1 - \hat{m}_q^2)/2 \leq \hat{E}_q \leq (1 - \hat{m}_q)$ then yields the branching ratio

$$\begin{aligned} \mathcal{B}(\bar{B} \rightarrow X_q \nu \bar{\nu}) &= \frac{\alpha^2}{4\pi^2 \sin^4 \theta_W} \frac{|V_{tb} V_{tq}^*|^2}{|V_{cb}|^2} \frac{\mathcal{B}(\bar{B} \rightarrow X_c e \bar{\nu}_e) \kappa(0)}{f(\hat{m}_c) \kappa(\hat{m}_c)} \\ &\times \sum_f \left\{ (|c_L|^2 + |c_R|^2) f(\hat{m}_q) - 4\text{Re}(c_L c_R^*) \hat{m}_q \tilde{f}(\hat{m}_q) \right\}, \end{aligned} \quad (5.7)$$

where

$$\tilde{f}(\hat{m}_q) = 1 + 9\hat{m}_q^2 - 9\hat{m}_q^4 - \hat{m}_q^6 + 12\hat{m}_q^2(1 + \hat{m}_q^2) \ln \hat{m}_q, \quad (5.8)$$

and $f(\hat{m}_q)$ is given in Eq. (5.3).

⁸Unlike the $b \rightarrow ql^+l^-$ transition, there is no virtual photon contribution in $b \rightarrow q\nu\bar{\nu}$, so that non-perturbative corrections due to charm quarks are further suppressed [44].

Table 1: Input parameters used in our numerical analysis. The isospin-breaking corrections r_K and the charm contributions $X_{\text{NL}} \equiv (2X_{\text{NL}}^e + X_{\text{NL}}^\tau)/3, Y_{\text{NL}}$ have been taken from Refs. [5] and [12], respectively. Note that m_c is the running charm quark mass in the $\overline{\text{MS}}$ scheme normalized at m_c . For the CKM matrix, we use the standard parametrization [41], with four independent parameters $s_{12}, s_{13}, s_{23}, \delta$. As for the remaining parameters, we utilize the values compiled by the Particle Data Group [42].

Quantity	Value
$\sin^2 \theta_W$	0.23
$\alpha_s(M_Z)$	0.118
s_{12}	0.222
s_{13}	3.49×10^{-3}
s_{23}	0.041
δ	57°
$ V_{td} $	7.81×10^{-3}
f_{B_s}	230 MeV
m_b^{pole}	4.8 GeV
m_t^{pole}	174.3 GeV
m_c	1.3 GeV
α	1/129
r_1	1.17×10^{-4}
r_2	0.24
r_3	13.17
r_{K^+}	0.901
r_{K_L}	0.944
X_{NL}	9.78×10^{-4}
Y_{NL}	3.03×10^{-4}
$\mathcal{B}(\bar{B} \rightarrow X_c e \bar{\nu}_e)$	10.58%

Table 2: Numerical values for the running quark masses $m_i \equiv m_i(\mu)$ employed in our analysis.

Scale	m_t [GeV]	m_s [MeV]	m_b [GeV]
$\mu = m_t^{\text{pole}}$	166	61	2.9
$\mu = m_b^{\text{pole}}$	—	90	4.4
$\mu = 2$ GeV	—	110	—

Thus far, no attempt has been made to search for the inclusive $b \rightarrow d\nu\bar{\nu}$ decay, and so we concentrate on the $b \rightarrow s$ transition. The best upper limit has been set by the ALEPH Collaboration [48]:⁹

$$\mathcal{B}(\bar{B} \rightarrow X_s \nu\bar{\nu}) < 6.4 \times 10^{-4} \quad (90\% \text{ C.L.}). \quad (5.9)$$

Using the numerical values listed in Tables 1 and 2, together with Eq. (5.6), we obtain

$$\begin{aligned} \mathcal{B}(\bar{B} \rightarrow X_s \nu\bar{\nu}) &= 5.39 \times 10^{-6} \left[\frac{0.53}{f(\hat{m}_c)} \right] \left[\frac{0.88}{\kappa(\hat{m}_c)} \right] \left[\frac{\mathcal{B}(\bar{B} \rightarrow X_c e\bar{\nu}_e)}{10.58\%} \right] \frac{|V_{ts}|^2}{|V_{cb}|^2} \\ &\times \sum_f (|c_L|^2 + |c_R|^2) \left[1 - 0.08 \frac{\text{Re}(c_L c_R^*)}{|c_L|^2 + |c_R|^2} \right], \end{aligned} \quad (5.10)$$

which will be used in the subsequent analysis. We note in passing that, since

$$-\frac{1}{2} \leq \frac{\text{Re}(c_L c_R^*)}{|c_L|^2 + |c_R|^2} \leq \frac{1}{2}, \quad (5.11)$$

the last term in square brackets in Eq. (5.10) deviates from unity by at most 4%. The SM result is obtained by summing over the neutrino flavours f , and taking the limit $c_R \rightarrow 0$ while retaining only the SM contribution in c_L . In this case, $c_L = X_{\text{SM}}$, with X_{SM} given in Eq. (A.1) of the Appendix.

5.1.2 $\bar{B}_{d,s} \rightarrow l^+l^-$

The decays $\bar{B}_q \rightarrow l^+l^-$ are after $\bar{B} \rightarrow X_q \nu\bar{\nu}$ the theoretically cleanest decays in the field of rare B decays. In fact, like in the decay $\bar{B} \rightarrow X_{d,s} \nu\bar{\nu}$, the charm contributions are completely negligible. These processes, which are dominated by Z^0 -penguin and box diagrams, have been studied by a number of authors [24–28, 51, 52] in extensions of the SM, but without QCD corrections.

Let us start by considering the matrix element for the decay $\bar{B}_q \rightarrow l^+l^-$ in the presence of the operators defined in Eqs. (3.28)–(3.30), which has the general form¹⁰

$$\mathcal{M} = -i f_{B_q} \frac{G_F \alpha}{\sqrt{2\pi} \sin^2 \theta_W} V_{tb} V_{tq}^* [F_S \bar{l}l + F_P \bar{l}\gamma_5 l + F_V p^\mu \bar{l}\gamma_\mu l + F_A p^\mu \bar{l}\gamma_\mu \gamma_5 l], \quad (5.12)$$

where the F_i 's are Lorentz-invariant form factors, p^μ is the four-momentum of the initial B meson, and f_{B_q} is the corresponding decay constant defined via the axial vector current matrix element

$$\langle 0 | \bar{q} \gamma_\mu \gamma_5 b | \bar{B}_q(p) \rangle = i p_\mu f_{B_q}, \quad (5.13)$$

⁹A similar upper limit has been derived by the CLEO Collaboration for the branching fraction $\mathcal{B}(B^\pm \rightarrow K^\pm \nu\bar{\nu}) < 2.4 \times 10^{-4}$ at 90% C.L. [49]. We do not address the issue of exclusive decays here (see, e.g., Refs. [50, 51]).

¹⁰Observe that there is no tensor-type interaction as $\langle 0 | \bar{q} \sigma_{\mu\nu} b | \bar{B}_q(p) \rangle \equiv 0$. In fact, it is not possible to construct a combination made up of p^μ that is antisymmetric with respect to the index interchange $\mu \leftrightarrow \nu$.

while the matrix element of the vector current vanishes. It may also be noted that the form factor F_V does not contribute to the decay $\bar{B}_q \rightarrow l^+l^-$ since $\bar{l}\not{l} = 0$. Employing the equation of motion, we find for the remaining matrix element

$$\langle 0 | \bar{q} \gamma_5 b | \bar{B}_q(p) \rangle = -i f_{B_q} \frac{M_{B_q}^2}{m_b + m_q}. \quad (5.14)$$

Squaring the matrix element and summing over the final lepton spins, the branching ratio can be written in a compact form [26]:

$$\mathcal{B}(\bar{B}_q \rightarrow l^+l^-) = \frac{G_F^2 \alpha^2 M_{B_q} f_{B_q}^2 \tau_{B_q}}{16\pi^3 \sin^4 \theta_W} |V_{tb} V_{tq}^*|^2 \sqrt{1 - \frac{4m_l^2}{M_{B_q}^2}} \left\{ \left(1 - \frac{4m_l^2}{M_{B_q}^2} \right) |F_S|^2 + |F_P + 2m_l F_A|^2 \right\}. \quad (5.15)$$

Here, τ_{B_q} is the lifetime of the B_q meson and

$$F_S = \frac{1}{2} M_{B_q}^2 \left[\frac{c_S - c'_S \hat{m}_q}{1 + \hat{m}_q} \right], \quad F_P = \frac{1}{2} M_{B_q}^2 \left[\frac{c_P - c'_P \hat{m}_q}{1 + \hat{m}_q} \right], \quad F_A = \frac{1}{2} (c_A - c'_A) \quad (5.16)$$

(remembering that $\hat{m}_q \equiv m_q/m_b$). At present, the best upper limit on the above decay modes comes from the Collider Detector at Fermilab (CDF) and has been derived for the $b \rightarrow s$ transition [53]:

$$\mathcal{B}(\bar{B}_s \rightarrow \mu^+ \mu^-) < 2.6 \times 10^{-6} \quad (95\% \text{ C.L.}), \quad (5.17)$$

and so we focus on the $\bar{B}_s \rightarrow \mu^+ \mu^-$ decay.

Recalling the scalar and pseudoscalar Wilson coefficients in Sec. 3.3, it turns out that the contributions of the operators $\mathcal{O}_{S,P}$ and $\mathcal{O}'_{S,P}$ are of comparable size. Thus, the Wilson coefficients $c'_{S,P}$ in Eq. (5.16) can be neglected since $\hat{m}_q \ll 1$ for $q = d, s$.

Introducing the dimensionless Wilson coefficients

$$\tilde{c}_S = M_{B_s} c_S, \quad \tilde{c}_P = M_{B_s} c_P, \quad (5.18)$$

the branching fraction is given by

$$\begin{aligned} \mathcal{B}(\bar{B}_s \rightarrow \mu^+ \mu^-) &= 2.32 \times 10^{-6} \left[\frac{\tau_{B_s}}{1.5 \text{ ps}} \right] \left[\frac{f_{B_s}}{230 \text{ MeV}} \right]^2 \left[\frac{|V_{ts}|}{0.040} \right]^2 \\ &\times [0.998 |\tilde{c}_S|^2 + |\tilde{c}_P + 0.039(c_A - c'_A)|^2], \end{aligned} \quad (5.19)$$

where we have set $\hat{m}_s = 0$ in Eq. (5.16) and used the input parameters shown in Tables 1 and 2. The SM result for the branching fraction may be obtained from Eq. (5.19) by setting $\tilde{c}_S = \tilde{c}_P = c'_A = 0$ and $c_A = -Y_{\text{SM}}$, with Y_{SM} defined in Eq. (A.2) of the Appendix.

5.2 Rare K decays

In this section we adopt a somewhat different notation from that of Refs. [12, 13, 35] in order to avoid high powers of $|V_{us}|$. That is, we define the ratios

$$r_1 = \frac{\alpha^2 \mathcal{B}(K^+ \rightarrow \pi^0 e^+ \nu_e)}{4\pi^2 \sin^4 \theta_W |V_{us}|^2} \frac{\tau_{K_L}}{\tau_{K^+}}, \quad r_2 = \frac{\tau_{K^+}}{\tau_{K_L}}, \quad r_3 = \frac{\mathcal{B}(K^+ \rightarrow \mu^+ \nu_\mu)}{\mathcal{B}(K^+ \rightarrow \pi^0 e^+ \nu_e)}, \quad (5.20)$$

with their numerical values summarized in Table 1.

5.2.1 $K^+ \rightarrow \pi^+ \nu \bar{\nu}$

Using the effective Hamiltonian in Eq. (3.60), it is straightforward to find the branching ratio for this decay. Since the matrix element of the operator \mathcal{O}_R equals the known matrix element of \mathcal{O}_L , we readily obtain the branching ratio from the formula given in Refs. [12, 13]:

$$\mathcal{B}(K^+ \rightarrow \pi^+ \nu \bar{\nu}) = 2r_1 r_2 r_{K^+} \sum_f \{[\text{Im } \lambda_t X(x)]^2 + [\text{Re } \lambda_c X_{\text{NL}} + \text{Re } \lambda_t X(x)]^2\}, \quad (5.21)$$

where the sum is over three neutrino species, r_{K^+} represents an isospin correction that one encounters when relating $K^+ \rightarrow \pi^+ \nu \bar{\nu}$ to $K^+ \rightarrow \pi^0 e^+ \nu_e$ [5], and $\lambda_i = V_{is}^* V_{id}$. The function

$$X_{\text{NL}} \equiv \frac{1}{3}(2X_{\text{NL}}^e + X_{\text{NL}}^\tau) \quad (5.22)$$

denotes the charm contributions discussed in Sec. 3.4, and

$$X = c_L + c_R \quad (5.23)$$

replaces the SM function X_{SM} given in Appendix A. The numerical values of $r_{1,2}$, r_{K^+} , and X_{NL} are given in Table 1.

As far as the current experimental situation is concerned, the first clean $K^+ \rightarrow \pi^+ \nu \bar{\nu}$ event was found by the E787 Collaboration [54]. Recently, further evidence for this decay mode has been reported in Ref. [55]. The updated branching ratio

$$\mathcal{B}(K^+ \rightarrow \pi^+ \nu \bar{\nu}) = (1.57^{+1.75}_{-0.82}) \times 10^{-10}, \quad (5.24)$$

being roughly by a factor of two higher than the SM expectation, provides already a non-trivial lower bound on V_{td} when interpreted within the SM framework [55, 56].

5.2.2 $K_L \rightarrow \pi^0 \nu \bar{\nu}$

The decay $K_L \rightarrow \pi^0 \nu \bar{\nu}$ is a short-distance dominated process that is largely governed by CP-violating contributions [7, 19, 57], and thus is sensitive only to the imaginary parts of the CKM couplings.¹¹ As the coupling $V_{cs}^* V_{cd}$ is real to an excellent approximation, the internal charm contributions can be completely neglected.

The $K_L \rightarrow \pi^0 \nu \bar{\nu}$ branching ratio may be obtained from the usual SM expression [12, 13] by replacing X_{SM} through X as defined in Eq. (5.23). Summing over neutrino flavours, we have

$$\mathcal{B}(K_L \rightarrow \pi^0 \nu \bar{\nu}) = 2r_1 r_{K_L} \sum_f [\text{Im} \lambda_t X(x)]^2, \quad (5.25)$$

where the isospin correction factor r_{K_L} is given in Table 1. The best current upper limit has been set by the KTeV Collaboration [58]:

$$\mathcal{B}(K_L \rightarrow \pi^0 \nu \bar{\nu}) < 5.9 \times 10^{-7} \text{ (90\% C.L.)}. \quad (5.26)$$

5.2.3 $K_L \rightarrow \mu^+ \mu^-$

As mentioned at the outset of the paper, the decay $K_L \rightarrow \mu^+ \mu^-$ suffers from theoretical uncertainties due to the long-distance dispersive contribution [15], and we therefore concentrate on the short-distance effects. In the part $\propto V_{ts}^* V_{td}$ only the SM operator \mathcal{O}_A has to be kept, as in the decays $K^+ \rightarrow \pi^+ \nu \bar{\nu}$ and $K_L \rightarrow \pi^0 \nu \bar{\nu}$, since the Wilson coefficients of the remaining operators are completely negligible. Likewise, in the part proportional to the CKM elements $V_{cs}^* V_{cd}$, non-negligible contributions arise only from \mathcal{O}_A .

Recalling $\lambda_i = V_{is}^* V_{id}$ and Eq. (5.20), the branching ratio may be written as

$$\mathcal{B}(K_L \rightarrow \mu^+ \mu^-)_{\text{SD}} = 4r_1 r_3 [\text{Re} \lambda_c Y_{\text{NL}} + \text{Re} \lambda_t Y(x)]^2, \quad (5.27)$$

where Y_{NL} represents the charm contribution obtained in Ref. [12] and $Y(x) = -c_A$. The numerical values of r_3 , as well as the remaining parameters, are listed in Tables 1 and 2.

6 Numerical analysis

In the subsequent analysis we will adopt the following procedure:

- We restrict our attention to the low and high $\tan \beta$ regime, as defined in Eq. (1.3). For the decays with a dilepton in the final state, we focus on the $\mu^+ \mu^-$ mode.

¹¹Strictly speaking, this does not pertain to models with lepton flavour violation, in which the CP-conserving amplitude can dominate [19].

- In the case of B decays, we will study the μ dependence of the various branching fractions only for those decay modes that are mediated by the $b \rightarrow s$ transition, which essentially involves the CKM element V_{ts} . It is important to emphasize that the presence of new-physics contributions may not only affect the decay modes under study but also $B_q^0 - \bar{B}_q^0$ mixing and the CP violation parameter ϵ_K , and consequently the extraction of the CKM elements V_{td} and V_{ts} . In this case, the standard analysis of the unitarity triangle may lead to false results. In fact, while to a good approximation $|V_{ts}| \approx |V_{cb}|$, independent of new-physics effects, the value of V_{td} determined using the SM formulae might differ from that obtained in the context of SUSY (see, e.g., Refs. [21, 33, 59]).

Since we are mainly interested in the μ dependence of the various branching fractions, rather than on their actual values, we fix $|V_{td}|$ to the SM value given in Table 1. Note that this treatment is different from the analysis of Ref. [21], where the new-physics effects on V_{td} have also been taken into account.

- The light quark masses, m_s and m_b , appearing in the Wilson coefficients are determined at the high-energy scale, but otherwise are evaluated at the low-energy scale (cf. Table 2). Since the contributions proportional to the down-quark mass are negligibly small, we may take $m_d = 0$.
- Our calculation is based on the assumption of minimal flavour violation, as outlined in Sec. 2. Furthermore, we assume that there are no new CP-violating phases in addition to the single phase residing in the CKM matrix.
- Since we ignore flavour-mixing effects among squarks, the matrix in Eq. (2.3) decomposes into three 2×2 matrices. A noticeable feature is that the LR terms are proportional to the masses of the up-type quarks. Hence, large mixing can occur in the scalar top quark sector, leading to a mass eigenstate, say, \tilde{t}_1 , possibly much lighter than the remaining squarks. We therefore keep LR mixing only in the stop sector, where the mass matrix is given by

$$M_{\tilde{t}}^2 = \begin{pmatrix} m_{\tilde{t}_L}^2 + m_t^2 + \frac{1}{6}M_Z^2 \cos 2\beta(3 - 4 \sin^2 \theta_W) & m_t(A_t - \mu \cot \beta) \\ m_t(A_t - \mu \cot \beta) & m_{\tilde{t}_R}^2 + m_t^2 + \frac{2}{3}M_Z^2 \cos 2\beta \sin^2 \theta_W \end{pmatrix}, \quad (6.1)$$

where $m_{\tilde{t}_{L,R}}$ are the soft SUSY breaking scalar masses and A_t is the trilinear coupling. In this framework, the mixing matrices Γ^{UL} and Γ^{UR} [Eq. (2.5)] take the simple form

$$(\Gamma^{UL})^T = \begin{pmatrix} 1 & 0 & 0 & 0 & 0 \\ 0 & 1 & 0 & 0 & 0 \\ 0 & 0 & \cos \theta_{\tilde{t}} & 0 & 0 \\ 0 & 0 & 0 & 0 & -\sin \theta_{\tilde{t}} \end{pmatrix}, \quad (\Gamma^{UR})^T = \begin{pmatrix} 0 & 0 & 1 & 0 & 0 \\ 0 & 0 & 0 & 1 & 0 \\ 0 & 0 & \sin \theta_{\tilde{t}} & 0 & 0 \\ 0 & 0 & 0 & 0 & \cos \theta_{\tilde{t}} \end{pmatrix}. \quad (6.2)$$

The physical mass eigenstates are then given by

$$\tilde{t}_1 = \cos \theta_{\tilde{t}} \tilde{t}_L + \sin \theta_{\tilde{t}} \tilde{t}_R, \quad \tilde{t}_2 = -\sin \theta_{\tilde{t}} \tilde{t}_L + \cos \theta_{\tilde{t}} \tilde{t}_R, \quad (6.3)$$

with the mixing angle ($-\pi/2 \leq \theta_{\tilde{t}} \leq \pi/2$)

$$\sin 2\theta_{\tilde{t}} = \frac{2m_t(A_t - \mu \cot \beta)}{m_{\tilde{t}_1}^2 - m_{\tilde{t}_2}^2}, \quad \cos 2\theta_{\tilde{t}} = \frac{(m_{\tilde{t}_L}^2 - m_{\tilde{t}_R}^2) + \frac{1}{6}M_Z^2 \cos 2\beta(3 - 8 \sin^2 \theta_W)}{m_{\tilde{t}_1}^2 - m_{\tilde{t}_2}^2}, \quad (6.4)$$

$m_{\tilde{t}_{1,2}}$ being the stop masses with $m_{\tilde{t}_1}^2 < m_{\tilde{t}_2}^2$. (The remaining up-type squark masses are taken to be equal.)

- For simplicity, we assume that the scalar partners of the leptons are degenerate in mass.
- For the results presented below we take into account the following lower bounds on the SUSY particle masses [42, 60, 61]:

$$m_{\tilde{t}_1, \tilde{b}_1} \gtrsim 100 \text{ GeV}, \quad m_{\tilde{q} \neq \tilde{t}_1, \tilde{b}_1} \gtrsim 260 \text{ GeV}, \quad m_{\tilde{l}, \tilde{\nu}} \gtrsim 100 \text{ GeV}, \quad M_{\tilde{\chi}_1} \gtrsim 100 \text{ GeV}. \quad (6.5)$$

As far as the lightest neutral Higgs boson, h^0 , is concerned, we must ensure that $M_{h^0} \geq 113.5 \text{ GeV}$ [61, 62], taking into account radiative corrections [63, 64] to the tree-level mass defined in Eq. (2.24).

Further restrictions on the SUSY parameter space are imposed by electroweak precision data such as the ρ parameter [42, 60, 65]. Also, we take into account the constraint on the trilinear coupling, A_t , arising from the requirement of the absence of colour and charge breaking minima [66].

- We require the various SUSY contributions to be consistent with the measured inclusive $b \rightarrow s\gamma$ branching fraction [67]. To be specific, we will allow the range of 2.0×10^{-4} to 4.5×10^{-4} for the branching ratio $\mathcal{B}(\bar{B} \rightarrow X_s \gamma)$. Besides, we take into account constraints on the Wilson coefficients arising from other rare exclusive B decays such as $\bar{B}_s \rightarrow \mu^+ \mu^-$ [Eq. (5.17)].

To determine the impact of the QCD corrections on the various branching ratios, we examine their μ dependence for given points in the SUSY parameter space. For definiteness, we have chosen the following SUSY parameter sets:

$$\tan \beta = 3: \quad \begin{cases} m_{\tilde{t}_1} = 200 \text{ GeV}, \quad m_{\tilde{t}_2} = 800 \text{ GeV}, \quad \theta_{\tilde{t}} = -70^\circ, \quad m_{\tilde{l}, \tilde{\nu}} = 100 \text{ GeV}, \\ M_H = 300 \text{ GeV}, \quad \mu = -300 \text{ GeV}, \quad M_2 = 800 \text{ GeV}, \quad M_{\tilde{g}} = 1 \text{ TeV}, \end{cases} \quad (6.6)$$

$$\tan \beta = 40: \begin{cases} m_{\tilde{t}_1} = 120 \text{ GeV}, m_{\tilde{t}_2} = 500 \text{ GeV}, \theta_{\tilde{t}} = -70^\circ, m_{\tilde{l}, \tilde{\nu}} = 100 \text{ GeV}, \\ M_H = 250 \text{ GeV}, \mu = -350 \text{ GeV}, M_2 = 800 \text{ GeV}, M_{\tilde{g}} = 1 \text{ TeV}, \end{cases} \quad (6.7)$$

$$\tan \beta = 40: \begin{cases} m_{\tilde{t}_1} = 500 \text{ GeV}, m_{\tilde{t}_2} = 650 \text{ GeV}, \theta_{\tilde{t}} = -44^\circ, m_{\tilde{l}, \tilde{\nu}} = 100 \text{ GeV}, \\ M_H = 200 \text{ GeV}, \mu = -600 \text{ GeV}, M_2 = 800 \text{ GeV}, M_{\tilde{g}} = 1 \text{ TeV}. \end{cases} \quad (6.8)$$

Note that in the case of $\theta_{\tilde{t}} = -70^\circ$ the lighter scalar top quark is predominantly right-handed [cf. Eq. (6.3)] while the choice $\theta_{\tilde{t}} = -44^\circ$ corresponds to a scenario with almost maximal mixing, i.e. $|\sin(2\theta_{\tilde{t}})| \approx 1$.

In Figs. 5–9 we summarize our results for the μ dependence of the branching ratios of $\bar{B} \rightarrow X_s \nu \bar{\nu}$, $\bar{B}_s \rightarrow \mu^+ \mu^-$, $K^+ \rightarrow \pi^+ \nu \bar{\nu}$, $K_L \rightarrow \pi^0 \nu \bar{\nu}$ and $K_L \rightarrow \mu^+ \mu^-$. Overall we see that the dependence of the various branching fractions on the renormalization scale is considerably reduced once QCD corrections are taken into account. In fact, the μ dependence inherent in the leading-order predictions, typically 10–20%, is reduced to a few per cent once $O(\alpha_s)$ corrections are taken into account.

Figures (5) and (6) show the μ dependence of the $\bar{B} \rightarrow X_s \nu \bar{\nu}$ branching ratio for the low and high $\tan \beta$ regime, respectively. Notice that the SUSY contributions interfere constructively or destructively with those of the SM, depending on our choice of SUSY parameters. Another noticeable feature is that the value of μ at which leading order (LO) and next-to-leading order (NLO) corrections coincide depends on whether one uses $\kappa = 1$ or κ according to Eqs. (5.5) and (5.6) in the LO expression for the $\bar{B} \rightarrow X_s \nu \bar{\nu}$ branching ratio.

Turning to the $\bar{B}_s \rightarrow \mu^+ \mu^-$ decay, we show in Figs. (7) and (8) the branching fraction for the low and high $\tan \beta$ regime, respectively. While in the former region the branching ratio in the SM is only mildly affected by the SUSY contributions (see Fig. 7), in the high $\tan \beta$ regime the supersymmetric effects can be enormous. This can be seen from Fig. 8 where we have plotted the branching ratio for the case of a predominantly right-handed light stop quark [Fig. 8(a)] and for the scenario of maximal mixing in the scalar top-quark sector [Fig. 8(b)]. Note that the value of μ at which the leading and next-to-leading order results for the branching ratio coincide depends on the choice of input parameters.

We should mention that the large new-physics effects in $\bar{B}_s \rightarrow \mu^+ \mu^-$ in the high $\tan \beta$ regime, compared to those in $\bar{B} \rightarrow X_s \nu \bar{\nu}$, are due to the fact that in the former decay mode the leading contribution scales roughly as $\sim m_b m_\mu \tan^3 \beta$ while in the latter decay it behaves as $\sim m_b m_s \tan^2 \beta$.

In Fig. 9 we have plotted the branching ratios for the decays $K_L \rightarrow \mu^+ \mu^-$, $K^+ \rightarrow \pi^+ \nu \bar{\nu}$ and $K_L \rightarrow \pi^0 \nu \bar{\nu}$ in the low $\tan \beta$ regime. For large values of $\tan \beta$ the SUSY contributions are negligibly small. As far as new operators are concerned, they do not give any sizable contributions, due to the suppression of the light quark masses.

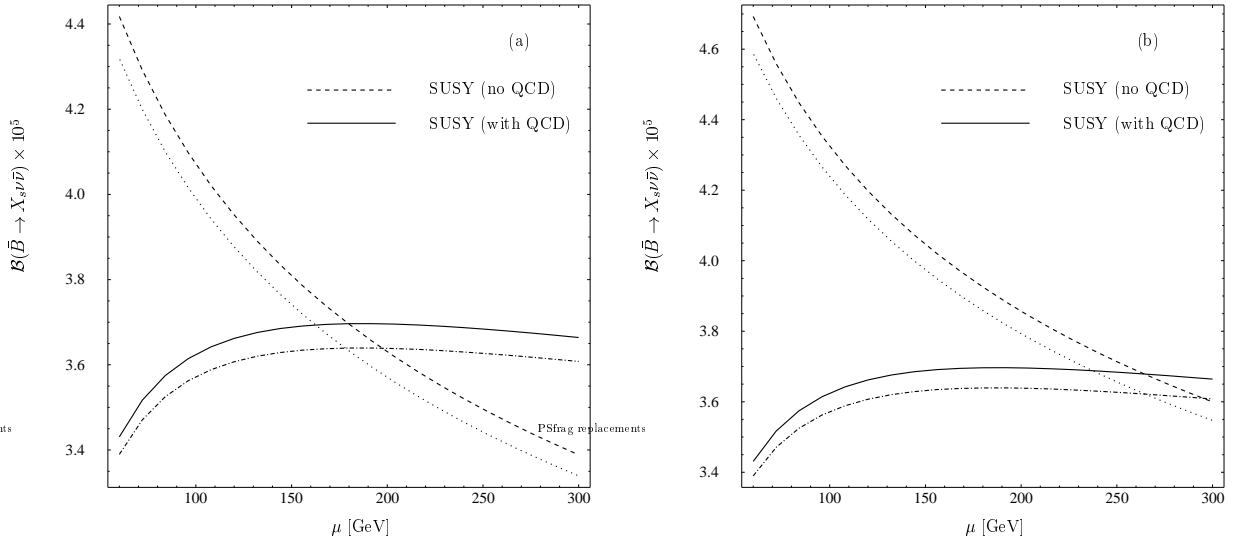


Figure 5: Predictions of the μ dependence of the $\bar{B} \rightarrow X_s \nu \bar{\nu}$ branching ratio obtained (a) using κ as given in Eqs. (5.5) and (5.6) in the leading order (LO) as well as the next-to-leading order (NLO) branching ratio [Eq. (5.7)], and (b) taking $\kappa = 1$ in the LO expression of the branching ratio. The solid (dashed) curves represent the SUSY results with (without) QCD corrections. We have chosen $\tan \beta = 3$, together with the parameter set given in Eq. (6.6). For comparison, we also show the SM prediction with (dash-dotted curve) and without (dotted curve) QCD corrections.

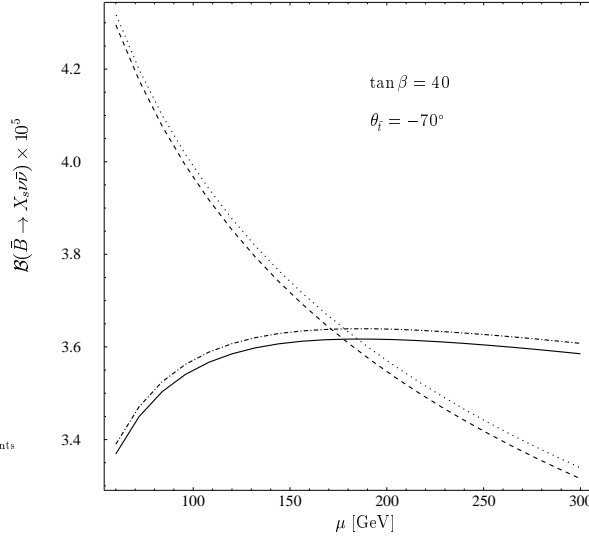


Figure 6: Branching ratio of the $\bar{B} \rightarrow X_s \nu \bar{\nu}$ decay vs the renormalization scale μ at large $\tan \beta$, as defined in Eq. (6.7). We have used κ according to Eqs. (5.5) and (5.6) in both the LO as well as the NLO expression for the branching ratio [Eq. (5.7)]. The legends are the same as in Fig. 5.

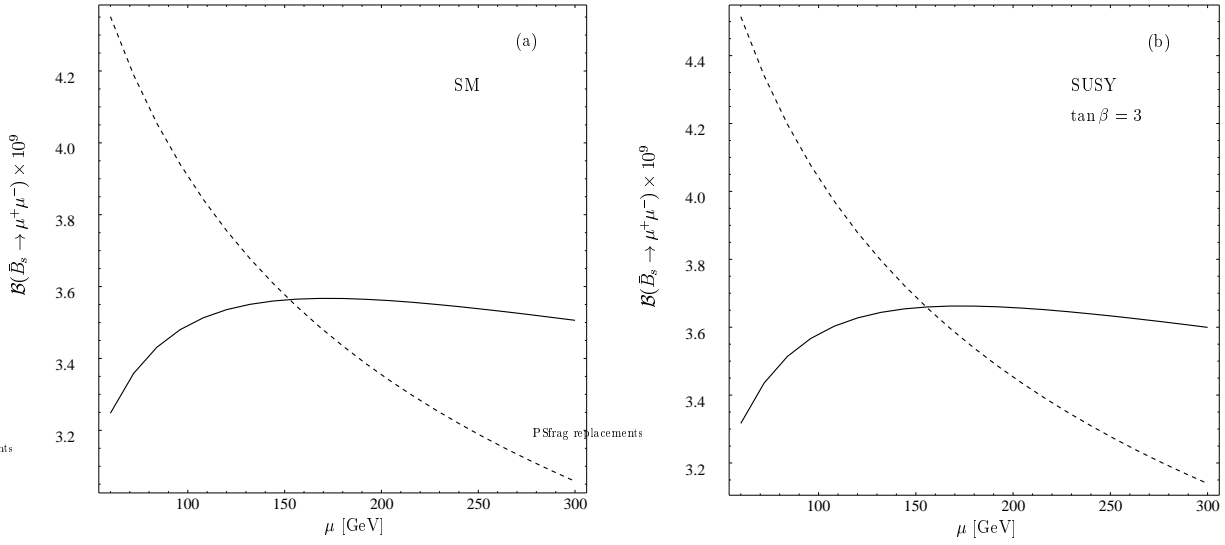


Figure 7: The μ dependence of the $\bar{B}_s \rightarrow \mu^+ \mu^-$ branching ratio for (a) the SM, and (b) SUSY in the low $\tan \beta$ regime, as defined in Eq. (6.6). The solid and dashed curves denote the predictions with and without QCD corrections, respectively.

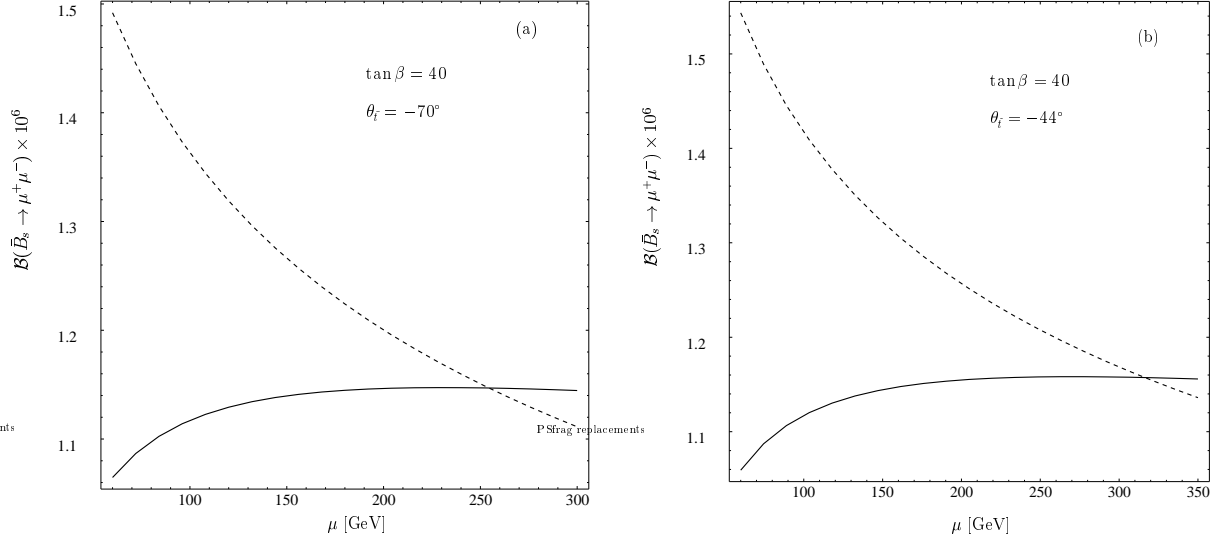


Figure 8: The μ dependence of the $\bar{B}_s \rightarrow \mu^+ \mu^-$ branching ratio within SUSY at large $\tan \beta$. The solid and dashed curves denote the SUSY prediction with and without QCD corrections, respectively. (a) For the case of a predominantly right-handed light stop quark, using the SUSY input parameters given in Eq. (6.7). (b) For the case of almost maximal mixing in the scalar top quark sector according to the parameter set given in Eq. (6.8). Note the order-of-magnitude enhancement of the branching ratio, compared to the SM and low $\tan \beta$ SUSY predictions in Fig. 7.

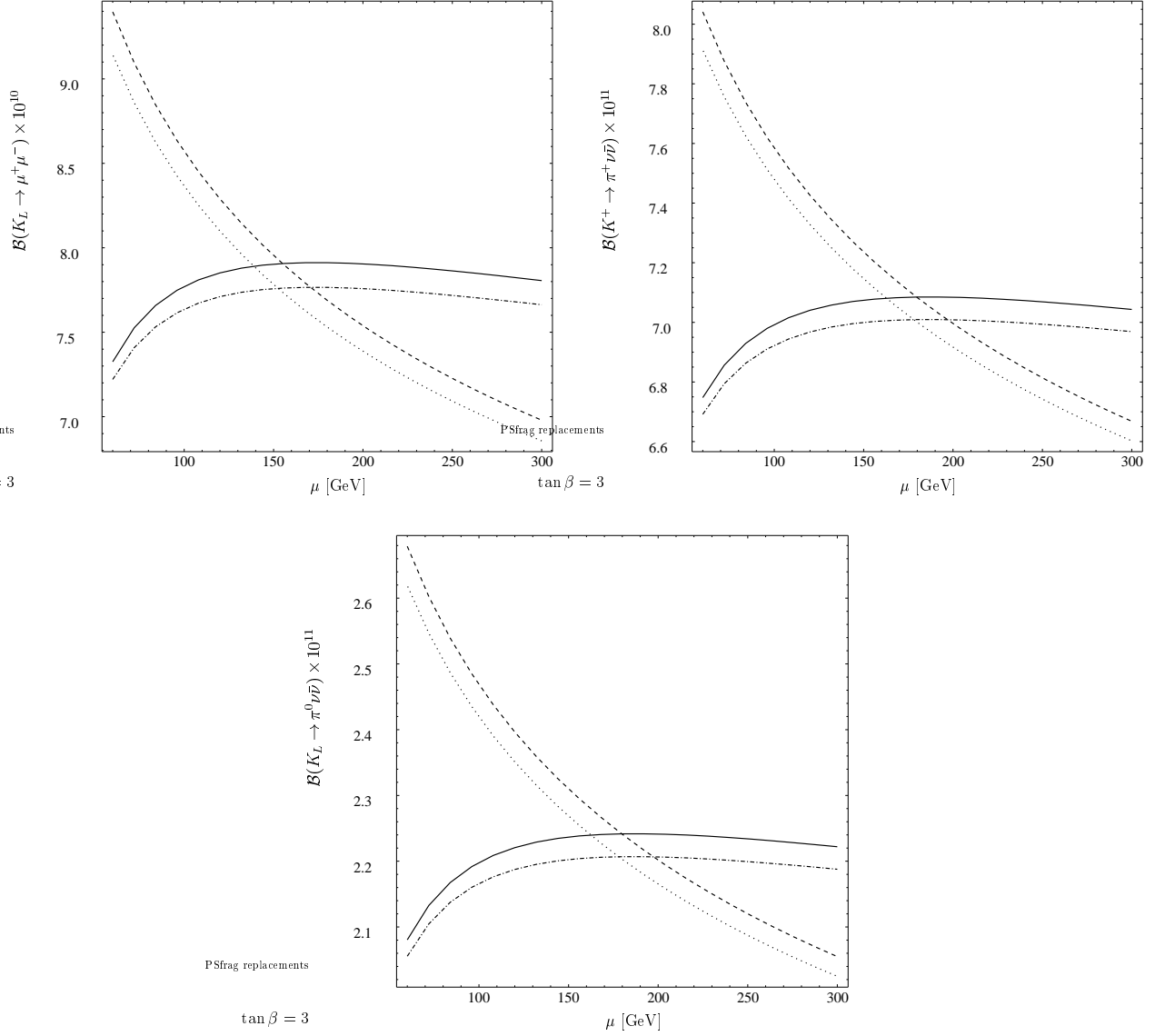


Figure 9: The $K_L \rightarrow \mu^+ \mu^-$, $K^+ \rightarrow \pi^+ \nu \bar{\nu}$ and $K_L \rightarrow \pi^0 \nu \bar{\nu}$ branching ratios, as a function of the renormalization scale μ . The dash-dotted (dotted) curves correspond to the SM prediction with (without) QCD corrections while the solid (dashed) curves denote the SUSY prediction with (without) QCD corrections. We have chosen $\tan \beta = 3$ along with the SUSY parameter set displayed in Eq. (6.6).

7 Corrections to the b -quark mass at large $\tan \beta$

Before summarizing, a few remarks are in order regarding corrections to the b quark Yukawa coupling, which may be important in the high $\tan \beta$ regime [24, 68]. As a matter of fact, sizable contributions to the down-type quarks, and hence to the CKM elements, may occur. Recently, it has been pointed out in Refs. [27, 28, 69, 70] that the corrections to the b quark Yukawa coupling, which are complementary to those presented in the preceding sections, can be substantial in rare B decays like $\bar{B}_s \rightarrow \mu^+ \mu^-$ and $b \rightarrow s\gamma$. Since our main emphasis has been on the μ dependence of the various branching ratios, rather than on their precise values, this issue will not be pursued here.

8 Summary and conclusions

We have carried out, for the first time, a calculation of QCD corrections to the branching ratios of the decays $\bar{B} \rightarrow X_{d,s}\nu\bar{\nu}$, $\bar{B}_{d,s} \rightarrow \mu^+ \mu^-$, $K^+ \rightarrow \pi^+ \nu\bar{\nu}$, $K_L \rightarrow \pi^0 \nu\bar{\nu}$ and $K_L \rightarrow \mu^+ \mu^-$ within SUSY. Our results are applicable to a version of the MSSM in which (a) the gluinos decouple; (b) flavour violation is governed exclusively by the CKM matrix; and (c) the neutralinos do not contribute.

Our main results can be summarized as follows:

- (i) We have provided a compendium of branching ratios and Wilson coefficients in the presence of supersymmetry, including all relevant dimension-six operators. Our results are valid for arbitrary values of $\tan \beta$ except for the neutral Higgs-boson contributions, which have been obtained in the high $\tan \beta$ regime.
- (ii) The inclusion of QCD corrections within the SM and SUSY leads to a significant reduction of the unphysical renormalization scale dependence, which is related to the running quark and squark masses, and which is unavoidably present in the existing leading-order formulae. While in the leading-order expression the scale uncertainty is typically 10–20% in the branching ratio, it is reduced to a few per cent after $O(\alpha_s)$ corrections are taken into account.
- (iii) For the set of SUSY parameters considered in this paper, it is possible to find a value of the renormalization scale μ for which the $O(\alpha_s)$ QCD corrections to the branching fractions are below, say, 2%, so that they can be neglected. In this case, one can estimate these QCD-corrected branching ratios merely by using the leading-order result with the proper choice of μ . Its actual value depends, of course, on the process considered, as well as on the specific choice of the SUSY parameters (see our discussion in Sec. 6).
- (iv) As far as new operators are concerned, our analysis implies that in the low $\tan \beta$ regime $2 \leq \tan \beta \leq 5$, only the SM operators are relevant, with their Wilson coefficients modified by

the presence of non-SM contributions. By contrast, in the large $\tan \beta$ region $40 \leq \tan \beta \leq 60$, the effects of new operators can lead to an order-of-magnitude enhancement in the decays $\bar{B}_{d,s} \rightarrow \mu^+ \mu^-$, in accordance with previous studies [24–28], and also provide substantial contributions to ΔM_{B_s} [28, 59]. As for the decays $\bar{B} \rightarrow X_{d,s} \nu \bar{\nu}$, the supersymmetric corrections due to new operators, although enhanced by powers of $\tan \beta$, are generally smaller since they are suppressed by the light quark masses $m_{d,s}$. Finally, the corresponding corrections in kaon decays are completely negligible.

Acknowledgements

We would like to thank Manuel Drees, Thorsten Ewerth, Mikołaj Misiak and Janusz Rosiek for useful discussions. This research was partially supported by the German ‘Bundesministerium für Bildung und Forschung’ under contract 05HT1WOA3 and by the ‘Deutsche Forschungsgemeinschaft’ (DFG) under contract Bu.706/1-1.

A Standard model notation

In this Appendix we give the correspondence of our results with the notation commonly used in the literature within the context of the SM. In this case, the decays $K_L \rightarrow \pi^0 \nu \bar{\nu}$, $\bar{B} \rightarrow X_q \nu \bar{\nu}$ and $\bar{B}_q \rightarrow l^+ l^-$ are described by the loop functions X_{SM} and Y_{SM} in the top-quark sector, which are defined as [1, 35]

$$X_{\text{SM}}(x) \equiv X_0(x) + \frac{\alpha_s}{4\pi} X_1(x) = C(x) - 4B(x, 1/2), \quad (\text{A.1})$$

$$Y_{\text{SM}}(x) \equiv Y_0(x) + \frac{\alpha_s}{4\pi} Y_1(x) = C(x) - B(x, -1/2), \quad (\text{A.2})$$

where C and B correspond to Z^0 -penguin and box-type contributions, respectively. In terms of the loop functions given in Appendix B, we find

$$C(x) = \frac{1}{4} \left\{ f_1^{(0)}(x) + \frac{\alpha_s}{4\pi} \left[f_1^{(1)}(x) + 8x \frac{\partial}{\partial x} f_1^{(0)}(x) \ln \left(\frac{\mu^2}{m_t^2} \right) \right] \right\}, \quad (\text{A.3})$$

$$B(x, 1/2) = \frac{1}{4} \left\{ f_2^{(0)}(x) + \frac{\alpha_s}{4\pi} \left[f_6^{(1)}(x) + 8x \frac{\partial}{\partial x} f_2^{(0)}(x) \ln \left(\frac{\mu^2}{m_t^2} \right) \right] \right\}, \quad (\text{A.4})$$

$$B(x, -1/2) = \frac{1}{4} \left\{ f_2^{(0)}(x) + \frac{\alpha_s}{4\pi} \left[f_{10}^{(1)}(x) + 8x \frac{\partial}{\partial x} f_2^{(0)}(x) \ln \left(\frac{\mu^2}{m_t^2} \right) \right] \right\}. \quad (\text{A.5})$$

The expressions in Eqs. (A.3)–(A.5) agree with the results found in Refs. [11, 12]. Note that in these papers the explicit μ dependence is given in terms of $\ln(\mu^2/M_W^2)$.

B Auxiliary functions

Defining the dilogarithm Li_2 by

$$\text{Li}_2(z) = - \int_0^z dt \frac{\ln(1-t)}{t}, \quad (\text{B.1})$$

the loop functions $f_p^{(0)}, f_{p'}^{(1)}$ appearing in the formulae of Sec. 3 have the following form:

$$f_1^{(0)}(x) = -\frac{x(6-x)}{2(x-1)} + \frac{x(2+3x)}{2(x-1)^2} \ln x, \quad (\text{B.2})$$

$$f_2^{(0)}(x) = -\frac{x}{x-1} + \frac{x}{(x-1)^2} \ln x, \quad (\text{B.3})$$

$$f_3^{(0)}(x, y) = \frac{x \ln x}{(x-1)(x-y)} + \frac{y \ln y}{(y-1)(y-x)}, \quad (\text{B.4})$$

$$f_4^{(0)}(x, y) = \frac{x^2 \ln x}{(x-1)(x-y)} + \frac{y^2 \ln y}{(y-1)(y-x)}, \quad (\text{B.5})$$

$$f_5^{(0)}(x, y, z) = \frac{x^2 \ln x}{(x-1)(x-y)(x-z)} + (x \leftrightarrow y) + (x \leftrightarrow z), \quad (\text{B.6})$$

$$f_6^{(0)}(x, y, z) = \frac{x \ln x}{(x-1)(x-y)(x-z)} + (x \leftrightarrow y) + (x \leftrightarrow z), \quad (\text{B.7})$$

$$f_7^{(0)}(x, y) = \frac{x \ln x}{(x-1)(x-y)} + \frac{x \ln y}{(y-1)(y-x)}, \quad (\text{B.8})$$

$$f_8^{(0)}(x) = \frac{x \ln x}{x-1}, \quad (\text{B.9})$$

$$f_9^{(0)}(w, x, y, z) = \frac{w^2 \ln w}{(w-1)(w-x)(w-y)(w-z)} + (w \leftrightarrow x) + (w \leftrightarrow y) + (w \leftrightarrow z), \quad (\text{B.10})$$

$$f_{10}^{(0)}(w, x, y, z) = \frac{w \ln w}{(w-1)(w-x)(w-y)(w-z)} + (w \leftrightarrow x) + (w \leftrightarrow y) + (w \leftrightarrow z), \quad (\text{B.11})$$

$$f_{11}^{(0)}(x, y) = \frac{x \ln x}{(x-y)} + \frac{x \ln y}{(y-x)}, \quad (\text{B.12})$$

$$f_1^{(1)}(x) = \frac{4x(29+7x+4x^2)}{3(x-1)^2} - \frac{4x(23+14x+3x^2)}{3(x-1)^3} \ln x - \frac{4x(4+x^2)}{(x-1)^2} \text{Li}_2\left(1 - \frac{1}{x}\right), \quad (\text{B.13})$$

$$f_2^{(1)}(x) = \frac{32x(3-x)}{3(x-1)^2} - \frac{8x(11-3x)}{3(x-1)^3} \ln x - \frac{8x(2-x)}{(x-1)^2} \text{Li}_2\left(1 - \frac{1}{x}\right), \quad (\text{B.14})$$

$$f_3^{(1)}(x, y) = -\frac{28y}{3(x-y)(y-1)} + \frac{2x(11x+3y)}{3(x-1)(x-y)^2} \ln x + \frac{2y[x(25-11y)-y(11+3y)]}{3(x-y)^2(y-1)^2} \ln y \\ + \frac{4(1+y)}{(x-1)(y-1)} \text{Li}_2\left(1-\frac{1}{y}\right) + \frac{4(x+y)}{(x-1)(x-y)} \text{Li}_2\left(1-\frac{x}{y}\right), \quad (\text{B.15})$$

$$f_4^{(1)}(x, y) = \frac{59x(1-y)-y(59-3y)}{6(y-1)(x-y)} + \frac{4x(7x^2-3xy+3y^2)}{3(x-1)(x-y)^2} \ln x + 2 \ln^2 y \\ + \frac{4y^2[x(18-11y)-y(11-4y)]}{3(x-y)^2(y-1)^2} \ln y \\ + \frac{4(1+y^2)}{(x-1)(y-1)} \text{Li}_2\left(1-\frac{1}{y}\right) + \frac{4(x^2+y^2)}{(x-1)(x-y)} \text{Li}_2\left(1-\frac{x}{y}\right), \quad (\text{B.16})$$

$$f_5^{(1)}(x, y) = -\frac{83+27x(y-1)-27y}{6(x-1)(y-1)} - \left\{ \frac{4x[1+x(12+y)-y-6x^2]}{3(x-1)^2(x-y)} \ln x \right. \\ - \frac{2[1+6x^2(y-1)-3x^3(y-1)+x(3y-4)]}{3(x-1)^2(x-y)(y-1)} \ln^2 x \\ + \frac{4y[3x^2(y-1)+xy(3-2y)+y^2(y-2)]}{3(x-1)(x-y)^2(y-1)} \text{Li}_2\left(1-\frac{x}{y}\right) \\ + \frac{4[1-3x-x^2(3-6y)-x^3]}{3(x-1)(x-y)(y-1)} \text{Li}_2\left(1-\frac{1}{x}\right) + (x \leftrightarrow y) \left. \right\} \\ + 4 \ln x \left(1 + x \frac{\partial}{\partial x} + y \frac{\partial}{\partial y} \right) f_4^{(0)}(x, y), \quad (\text{B.17})$$

$$f_6^{(1)}(x) = \frac{2x(29+3x)}{3(x-1)^2} - \frac{2x(25+7x)}{3(x-1)^3} \ln x - \frac{8x}{(x-1)^2} \text{Li}_2\left(1-\frac{1}{x}\right), \quad (\text{B.18})$$

$$f_7^{(1)}(x) = \frac{4x[27-11x+(x-1)^2\pi^2]}{3(x-1)^2} - \frac{4x(37-33x+12x^2)}{3(x-1)^3} \ln x \\ - \frac{8x(2-2x+x^2)}{(x-1)^2} \text{Li}_2\left(1-\frac{1}{x}\right), \quad (\text{B.19})$$

$$f_8^{(1)}(x, y, z) = -\frac{28y^2}{3(x-y)(y-1)(y-z)} + \left[\frac{4x(7x^2-3xy+3y^2)}{3(x-1)(x-y)^2(x-z)} \ln x + (x \leftrightarrow z) \right] \\ - \frac{4y^2\{x[4y^2+18z-11y(1+z)+y[3y^2-11z+4y(1+z)]\}}{3(x-y)^2(y-1)^2(y-z)^2} \ln y \\ - \frac{4(1+y^2)}{(x-1)(y-1)(z-1)} \text{Li}_2\left(1-\frac{1}{y}\right) \\ + \left[\frac{4(x^2+y^2)}{(x-1)(x-y)(x-z)} \text{Li}_2\left(1-\frac{x}{y}\right) + (x \leftrightarrow z) \right], \quad (\text{B.20})$$

$$\begin{aligned}
f_9^{(1)}(x, y, z) = & -\frac{28y}{3(x-y)(y-1)(y-z)} + \left[\frac{2x(11x+3y)}{3(x-1)(x-y)^2(x-z)} \ln x + (x \leftrightarrow z) \right] \\
& + \frac{2y\{x[3y^2-25z+11y(1+x)]+y[11z-17y^2+3y(1+z)]\}}{3(x-y)^2(y-1)^2(y-z)^2} \ln y \\
& - \frac{4(1+y)}{(x-1)(y-1)(z-1)} \text{Li}_2\left(1-\frac{1}{y}\right) \\
& + \left[\frac{4(x+y)}{(x-1)(x-y)(x-z)} \text{Li}_2\left(1-\frac{x}{y}\right) + (x \leftrightarrow z) \right], \tag{B.21}
\end{aligned}$$

$$f_{10}^{(1)}(x) = \frac{4x(19-3x)}{3(x-1)^2} - \frac{4x(17-x)}{3(x-1)^3} \ln x - \frac{8x}{(x-1)^2} \text{Li}_2\left(1-\frac{1}{x}\right), \tag{B.22}$$

$$\begin{aligned}
f_{11}^{(1)}(x, y) = & \frac{4x[8y+(x-1)(x-y)\pi^2]}{3y(x-1)(x-y)} - \frac{8x[x^2-7y+3x(1+y)]}{3(x-y)^2(x-1)^2} \ln x \\
& - \frac{8x(3x-7y)}{3(x-y)^2(y-1)} \ln y - \frac{8x}{y-1} \text{Li}_2\left(1-\frac{1}{x}\right) + \frac{8x}{y(y-1)} \text{Li}_2\left(1-\frac{y}{x}\right), \tag{B.23}
\end{aligned}$$

$$\begin{aligned}
f_{12}^{(1)}(x, y, z) = & -\frac{28y^2}{3(x-y)(y-1)(y-z)} + \left[\frac{4x^2(6x+y)}{3(x-1)(x-y)^2(x-z)} \ln x + (x \leftrightarrow z) \right] \\
& - \frac{4y^2\{x[6y^2+20z-13y(1+z)]+y[y^2-13z+6y(1+z)]\}}{3(x-y)^2(y-1)^2(y-z)^2} \ln y, \tag{B.24}
\end{aligned}$$

$$\begin{aligned}
f_{13}^{(1)}(x, y, z) = & -\frac{28y}{3(x-y)(y-1)(y-z)} + \left[\frac{4x(6x+y)}{3(x-1)(x-y)^2(x-z)} \ln x + (x \leftrightarrow z) \right] \\
& + \frac{4y\{x[y^2-13z+6y(1+z)]+y[y-8y^2+6z+yz]\}}{3(x-y)^2(y-1)^2(y-z)^2} \ln y, \tag{B.25}
\end{aligned}$$

$$\begin{aligned}
f_{14}^{(1)}(x, y) = & \frac{32x^2}{3(x-1)(x-y)} - \frac{8x^2[7x(1+y)-11y-3x^2]}{3(x-1)^2(x-y)^2} \ln x \\
& - \frac{8xy(3x-7y)}{3(x-y)^2(y-1)} \ln y - \frac{8x}{y-1} \text{Li}_2\left(1-\frac{1}{x}\right) + \frac{8x}{y-1} \text{Li}_2\left(1-\frac{y}{x}\right), \tag{B.26}
\end{aligned}$$

$$f_{15}^{(1)}(x) = \frac{1-3x}{x-1} + \frac{2x}{(x-1)^2} \ln x + \frac{2x}{(x-1)} \text{Li}_2\left(1-\frac{1}{x}\right), \tag{B.27}$$

$$f_{16}^{(1)}(x) = \frac{28}{3(x-1)} - \frac{4x(13-6x)}{3(x-1)^2} \ln x, \tag{B.28}$$

$$f_{17}^{(1)}(x, y) = -\frac{28}{3(x-1)(y-1)} + \frac{4y(10-3y)}{3(x-y)(y-1)^2} \ln y - \frac{4y}{(x-y)(y-1)^2} \ln^2 y \\ + \left[\frac{4(13x-6x^2-3y-7xy+3x^2y)}{3(x-1)^2(x-y)(y-1)} + \frac{4y \ln y}{(x-y)(y-1)^2} \right] \ln x, \quad (\text{B.29})$$

$$f_{18}^{(1)}(x, y) = -\frac{28y}{3(x-y)(y-1)} + \frac{4x(6x+y)}{3(x-1)(x-y)^2} \ln x - \frac{4y[y(6+y)-x(13-6y)]}{3(x-y)^2(y-1)^2} \ln y, \quad (\text{B.30})$$

$$f_{19}^{(1)}(x, y) = -\frac{28[x(y-1)+y]}{3(x-y)(y-1)} + \frac{4x^2(6x+y)}{3(x-1)(x-y)^2} \ln x + \frac{4y^2[x(20-13y)-y(13-6y)]}{3(x-y)^2(y-1)^2} \ln y. \quad (\text{B.31})$$

References

- [1] A. J. Buras, in *Flavour Dynamics: CP Violation and Rare Decays*, Lectures given at International School of Subnuclear Physics, Erice, Italy, 2000, hep-ph/0101336.
- [2] G. Buchalla, in *Kaon and Charm Physics: Theory*, Lectures given at TASI 2000, Boulder, CO, 2000, hep-ph/0103166.
- [3] L. S. Littenberg, hep-ex/0010048.
- [4] G. Isidori, Talk given at *XX International Symposium on Lepton and Photon Interactions at High Energies*, July 23–28, 2001, Rome, Italy, hep-ph/0110255.
- [5] W. J. Marciano and Z. Parsa, *Phys. Rev.* **D53** (1996) R1.
- [6] D. Rein and L. M. Sehgal, *Phys. Rev.* **D39** (1989) 3325; J. S. Hagelin and L. S. Littenberg, *Prog. Part. Nucl. Phys.* **23** (1989) 1; M. Lu and M. B. Wise, *Phys. Lett.* **B324** (1994) 461; C. Q. Geng, I. J. Hsu and Y. C. Lin, *ibid.* **B355** (1995) 569; *Phys. Rev.* **D54** (1996) 877; S. Fajfer, *Nuovo Cimento* **110A** (1997) 397.
- [7] G. Buchalla and G. Isidori, *Phys. Lett.* **B440** (1998) 170.
- [8] A. F. Falk, A. Lewandowski and A. A. Petrov, *Phys. Lett.* **B505** (2001) 107.
- [9] G. Buchalla and A. J. Buras, *Nucl. Phys.* **B398** (1993) 285.
- [10] G. Buchalla and A. J. Buras, *Nucl. Phys.* **B400** (1993) 225.

- [11] M. Misiak and J. Urban, *Phys. Lett.* **B451** (1999) 161.
- [12] G. Buchalla and A. J. Buras, *Nucl. Phys.* **B548** (1999) 309.
- [13] G. Buchalla and A. J. Buras, *Nucl. Phys.* **B412** (1994) 106.
- [14] L. M. Sehgal, *Nuovo Cimento* **45A** (1966) 785; *Phys. Rev.* **183** (1969) 1511; *ibid.* **D4** (1971) 1582 (E).
- [15] L. Bergström, E. Massó and P. Singer, *Phys. Lett.* **B131** (1983) 229; *ibid.* **B249** (1990) 141; G. D'Ambrosio, G. Isidori and J. Portolés, *ibid.* **B423** (1998) 385; D. Gómez Dumm and A. Pich, *Phys. Rev. Lett.* **80** (1998) 4633; G. Valencia, *Nucl. Phys.* **B517** (1998) 339.
- [16] See, for example, H. P. Nilles, *Phys. Rep.* **110** (1984) 1; J. F. Gunion, H. E. Haber, G. L. Kane and S. Dawson, *The Higgs Hunter's Guide* (Addison-Wesley, Reading, MA, 1990); hep-ph/9302272 (E); S. P. Martin, hep-ph/9709356.
- [17] H. E. Haber and G. L. Kane, *Phys. Rep.* **117** (1985) 75; J. F. Gunion and H. E. Haber, *Nucl. Phys.* **B272** (1986) 1; *ibid.* **B402** (1993) 567 (E).
- [18] Y. Grossman, Z. Ligeti and E. Nardi, *Nucl. Phys.* **B465** (1996) 369; *ibid.* **B480** (1996) 753 (E).
- [19] Y. Grossman and Y. Nir, *Phys. Lett.* **B398** (1997) 163.
- [20] Y. Nir and M. P. Worah, *Phys. Lett.* **B423** (1998) 319; A. J. Buras, A. Romanino and L. Silvestrini, *Nucl. Phys.* **B520** (1998) 3; G. Colangelo and G. Isidori, *J. High Energy Phys.* **09** (1998) 009; T. Goto, Y. Okada and Y. Shimizu, *Phys. Rev.* **D58** (1998) 094006; G. C. Cho, *Eur. Phys. J.* **C5** (1998) 525; A. J. Buras, G. Colangelo, G. Isidori, A. Romanino and L. Silvestrini, *Nucl. Phys.* **B566** (2000) 3.
- [21] A. J. Buras, P. Gambino, M. Gorbahn, S. Jäger and L. Silvestrini, *Nucl. Phys.* **B592** (2001) 55.
- [22] S. Bertolini, F. Borzumati, A. Masiero and G. Ridolfi, *Nucl. Phys.* **B353** (1991) 591.
- [23] P. Cho, M. Misiak and D. Wyler, *Phys. Rev.* **D54** (1996) 3329.
- [24] K. S. Babu and C. Kolda, *Phys. Rev. Lett.* **84** (2000) 228.
- [25] P. H. Chankowski and Ł. Sławianowska, *Phys. Rev.* **D63** (2001) 054012; C. S. Huang, W. Liao, Q. S. Yan and S. H. Zhu, *ibid.* **D63** (2001) 114021; *ibid.* **D64** (2001) 059902 (E).
- [26] C. Bobeth, T. Ewerth, F. Krüger and J. Urban, *Phys. Rev.* **D64** (2001) 074014.

- [27] A. Dedes, H. K. Dreiner and U. Nierste, *Phys. Rev. Lett.* **87** (2001) 251804.
- [28] G. Isidori and A. Retico, *J. High Energy Phys.* **11** (2001) 001.
- [29] F. Krüger and J. C. Romão, *Phys. Rev.* **D62** (2000) 034020.
- [30] M. Misiak, S. Pokorski and J. Rosiek, in *Heavy Flavours II*, edited by A. J. Buras and M. Lindner (World Scientific, Singapore, 1998), p. 795 [hep-ph/9703442].
- [31] J. Rosiek, *Phys. Rev.* **D41** (1990) 3464; hep-ph/9511250 (E).
- [32] C. Bobeth, M. Misiak and J. Urban, *Nucl. Phys.* **B567** (2000) 153.
- [33] M. Ciuchini, G. Degrassi, P. Gambino and G. F. Giudice, *Nucl. Phys.* **B534** (1998) 3.
- [34] S. L. Glashow, J. Iliopoulos and L. Maiani, *Phys. Rev.* **D2** (1970) 1285.
- [35] G. Buchalla, A. J. Buras and M. E. Lautenbacher, *Rev. Mod. Phys.* **68** (1996) 1125.
- [36] A. J. Buras, in *Probing the Standard Model of Particle Interactions*, edited by R. Gupta *et al.* (Elsevier Science B.V., New York, 1999), p. 281 [hep-ph/9806471].
- [37] A. Djouadi, P. Gambino, S. Heinemeyer, W. Hollik, C. Jünger and G. Weiglein, *Phys. Rev.* **D57** (1998) 4179.
- [38] A. J. Buras, A. Kwiatkowski and N. Pott, *Nucl. Phys.* **B517** (1998) 353.
- [39] A. J. Buras, M. Misiak and J. Urban, *Nucl. Phys.* **B586** (2000) 397.
- [40] M. Jamin and A. Pich, *Nucl. Phys.* **B425** (1994) 15.
- [41] L.-L. Chau and W.-Y. Keung, *Phys. Rev. Lett.* **53** (1984) 1802.
- [42] Particle Data Group, D. E. Groom *et al.*, *Eur. Phys. J.* **C15** (2000) 1.
- [43] A. F. Falk, M. Luke and M. J. Savage, *Phys. Rev.* **D49** (1994) 3367; A. Ali, G. Hiller, L. T. Handoko and T. Morozumi, *ibid.* **D55** (1997) 4105; G. Buchalla and G. Isidori, *Nucl. Phys.* **B525** (1998) 333.
- [44] G. Buchalla, G. Isidori and S. J. Rey, *Nucl. Phys.* **B511** (1998) 594.
- [45] J. W. Chen, G. Rupak and M. J. Savage, *Phys. Lett.* **B410** (1997) 285.
- [46] N. Cabibbo and L. Maiani, *Phys. Lett.* **79B** (1978) 109.

- [47] Y. Nir, *Phys. Lett.* **B221** (1989) 184; A. F. Falk, M. Luke and M. J. Savage, *Phys. Rev.* **D53** (1996) 2491.
- [48] ALEPH Collaboration, R. Barate *et al.*, *Eur. Phys. J.* **C19** (2001) 213.
- [49] CLEO Collaboration, T. Browder *et al.*, hep-ex/0007057.
- [50] P. Colangelo, F. De Fazio, P. Santorelli and E. Scrimieri, *Phys. Lett.* **B395** (1997) 339; D. Melikhov, N. Nikitin and S. Simula, *ibid.* **B428** (1998) 171; T. M. Aliev and C. S. Kim, *Phys. Rev.* **D58** (1998) 013003; C. S. Kim, Y. G. Kim and T. Morozumi, *ibid.* **D60** (1999) 094007; T. M. Aliev, A. Özpineci and M. Savci, *Phys. Lett.* **B506** (2001) 77.
- [51] G. Buchalla, G. Hiller and G. Isidori, *Phys. Rev.* **D63** (2001) 014015.
- [52] W. Skiba and J. Kalinowski, *Nucl. Phys.* **B404** (1993) 3; Y. Grossman, Z. Ligeti and E. Nardi, *Phys. Rev.* **D55** (1997) 2768; D. Guetta and E. Nardi, *ibid.* **D58** (1998) 012001; H. E. Logan and U. Nierste, *Nucl. Phys.* **B586** (2000) 39.
- [53] CDF Collaboration, F. Abe *et al.*, *Phys. Rev.* **D57** (1998) 3811.
- [54] E787 Collaboration, S. Adler *et al.*, *Phys. Rev. Lett.* **84** (2000) 3768.
- [55] E787 Collaboration, S. Adler *et al.*, hep-ex/0111091.
- [56] G. D'Ambrosio and G. Isidori, hep-ph/0112135.
- [57] L. S. Littenberg, *Phys. Rev.* **D39** (1989) 3322.
- [58] KTeV Collaboration, A. Alavi-Harati *et al.*, *Phys. Rev.* **D61** (2000) 072006.
- [59] A. J. Buras, P. H. Chankowski, J. Rosiek and Ł. Sławianowska, *Nucl. Phys.* **B619** (2001) 434.
- [60] A. Djouadi, M. Drees and J. L. Kneur, *J. High Energy Phys.* **08** (2001) 055.
- [61] For a recent review, see G. G. Hanson, Talk given at *XX International Symposium on Lepton and Photon Interactions at High Energies*, July 23–28, 2001, Rome, Italy, hep-ex/0111058.
- [62] LEP Higgs Working Group, hep-ex/0107030.
- [63] J. Ellis, G. Ridolfi and F. Zwirner, *Phys. Lett.* **B262** (1991) 477; J. L. Lopez and D. V. Nanopoulos, *ibid.* **B266** (1991) 397; A. Dabelstein, *Z. Phys.* **C67** (1995) 495.

- [64] R. Hempfling and A. H. Hoang, *Phys. Lett.* **B331** (1994) 99; M. Carena, P. H. Chankowski, S. Pokorski and C. E. M. Wagner, *ibid.* **B441** (1998) 205; S. Heinemeyer, W. Hollik and G. Weiglein, *ibid.* **B455** (1999) 179; hep-ph/0002213; M. Carena, H. E. Haber, S. Heinemeyer, W. Hollik, C. E. M. Wagner and G. Weiglein, *Nucl. Phys.* **B580** (2000) 29.
- [65] M. Drees and K. Hagiwara, *Phys. Rev.* **D42** (1990) 1709; P. H. Chankowski, A. Dabelstein, W. Hollik, W. M. Mösle, S. Pokorski and J. Rosiek, *Nucl. Phys.* **B417** (1994) 101; J. Erler and D. M. Pierce, *ibid.* **B526** (1998) 53; A. Djouadi *et al.*, hep-ph/0002258.
- [66] J. M. Frère, D. R. T. Jones and S. Raby, *Nucl. Phys.* **B222** (1983) 11; M. Claudson, L. J. Hall and I. Hinchliffe, *ibid.* **B228** (1983) 501; A. Kusenko, P. Langacker and G. Segrè, *Phys. Rev.* **D54** (1996) 5824; J. A. Casas and S. Dimopoulos, *Phys. Lett.* **B387** (1996) 107.
- [67] ALEPH Collaboration, R. Barate *et al.*, *Phys. Lett.* **B429** (1998) 169; Belle Collaboration, K. Abe *et al.*, *ibid.* **B511** (2001) 151; CLEO Collaboration, S. Chen *et al.*, *Phys. Rev. Lett.* **87** (2001) 251807.
- [68] L. J. Hall, R. Rattazzi and U. Sarid, *Phys. Rev.* **D50** (1994) 7048; M. Carena, M. Olechowski, S. Pokorski and C. E. M. Wagner, *Nucl. Phys.* **B426** (1994) 269; R. Hempfling, *Z. Phys.* **C63** (1994) 309; T. Blažek, S. Raby and S. Pokorski, *Phys. Rev.* **D52** (1995) 4151.
- [69] M. Carena, D. Garcia, U. Nierste and C. E. M. Wagner, *Nucl. Phys.* **B577** (2000) 88; *Phys. Lett.* **B499** (2001) 141.
- [70] G. Degrassi, P. Gambino and G. F. Giudice, *J. High Energy Phys.* **12** (2000) 009.